



Recent Advancements on Three-Dimensional Electrospun Nanofiber Scaffolds for Tissue Engineering

Yujie Chen¹ · Xutao Dong² · Muhammad Shafiq¹ · Gregory Myles² · Norbert Radacsi² · Xiumei Mo¹

Received: 22 March 2022 / Accepted: 19 April 2022 / Published online: 16 May 2022
© Donghua University, Shanghai, China 2022

Abstract

Electrospinning is widely accepted as a technique for the fabrication of nanofibrous three-dimensional (3D) scaffolds which mimic extracellular matrix (ECM) microenvironment for tissue engineering (TE). Unlike normal densely-packed two-dimensional (2D) nanofibrous membranes, 3D electrospun nanofiber scaffolds are dedicated to more precise spatial control, endowing the scaffolds with a sufficient porosity and 3D environment similar to the *in vivo* settings as well as optimizing the properties, including injectability, compressibility, and bioactivity. Moreover, the 3D morphology regulates cellular interaction and mediates growth, migration, and differentiation of cell for matrix remodeling. The variation among scaffold structures, functions and applications depends on the selection of electrospinning materials and methods as well as on the post-processing of electrospun scaffolds. This review summarizes the recent new forms for building electrospun 3D nanofiber scaffolds for TE applications. A variety of approaches aimed at the fabrication of 3D electrospun scaffolds, such as multilayering electrospinning, sacrificial agent electrospinning, wet electrospinning, ultrasound-enhanced electrospinning as well as post-processing techniques, including gas foaming, ultrasonication, short fiber assembly, 3D printing, electrospaying, and so on are discussed, along with their advantages, limitations and applications. Meanwhile, the current challenges and prospects of 3D electrospun scaffolds are rationally discussed, providing an insight into developing the vibrant fields of biomedicine.

Keywords Electrospun · Nanofibers · Three-dimensional · Tissue engineering · Regenerative medicine · Scaffold · Polymer

Yujie Chen and Xutao Dong contributed equally.

S.I. : Fiber Materials for advanced applications.

-
- ✉ Muhammad Shafiq
shafiqdr786@yahoo.com
 - ✉ Norbert Radacsi
N.Radacsi@ed.ac.uk
 - ✉ Xiumei Mo
xmm@dhu.edu.cn

¹ Shanghai Engineering Research Center of Nano-Biomaterials and Regenerative Medicine, State Key Laboratory for Modification of Chemical Fibers and Polymer Materials, College of Chemistry, Chemical Engineering and Biotechnology, Donghua University, Songjiang, Shanghai 201600, China

² School of Engineering, Institute for Materials and Processes, The University of Edinburgh, King's Buildings, Edinburgh EH9 3FB, United Kingdom

Introduction

Tissue-engineered scaffolds serve as a substitute for the native extracellular matrix (ECM) and provide temporary support for tissue regeneration [1]. In addition to meeting the basic requirements, including biocompatibility, biodegradability and appropriate mechanical performance, high specific surface area, and interconnected porous structures are essential for scaffolds [2]. Three-dimensional (3D) scaffolds with a fibrillar framework mimic *in vivo* ECM microenvironments and hold great promise for bio-related fields [3]. A series of strategies has been opted for the fabrication of nanofibrillar scaffolds, such as self-assembly, phase separation, and electrospinning [4–6]. Amongst, electrospinning is a simple, inexpensive, versatile, and an evolving technology that has garnered widespread attention from academia and the industry for tissue engineering (TE) [7, 8]. With the advancement of nanotechnology, many electrospinning protocols and materials have been researched and refined to fabricate tailored 3D scaffolds [9].

The basic principle of electrospinning involves an electrodynamic process, where a liquid droplet is elongated and stretched into a continuous fiber through an applied electric field [10]. The major components in the electrospinning setup include a syringe pump, a needle, a reservoir of electrospinning solution, a grounded collector, and a high voltage power supply. During electrospinning, the droplet is extruded out from the tip of the needle/spinneret at a constant rate. Upon applying a high voltage between the tip of the needle and the grounded collector, the electrostatic repulsion from the accumulated liquid surface charges overcomes surface tension and forces the droplet into a Taylor cone shape. Once this Taylor cone is formed, a charged jet is ejected and extended into fine fibers that solidify and deposit onto the grounded collector [11]. The diameter of these fibers typically varies from tens of nanometers to a few micrometers. Alternatively, components in the basic electrospinning setup could be modified or combined with other novel technologies to realize different fibers' morphology or to circumvent problems that may arise in the simple setup [12]. While electrospinning membranes allow for the transport of nutrients and growth factors, cellular infiltration is generally restricted due to the extremely small pore size of the conventional two-dimensional (2D) membranes. This limitation also leads to non-uniform cell distribution and impedes tissue ingrowth. Therefore, 3D structures are extremely important for successful tissue reconstruction.

Electrospinning has been proved to be promising for fabricating 3D scaffolds for TE and shown to produce continuous and ultrathin polymeric fibers in various hierarchical patterns [13]. The 3D scaffolds may further allow for the fabrication of bio-artificial tissues and organs for regenerative medicine and other biomedical sectors [14]. The desired living cells are seeded into 3D scaffolds that are biodegradable and can replace tissues with similar biological and mechanical properties. Tissues are made up of groups of cells embedded within an ECM microenvironment working synergistically to provide the essential physical scaffolding for tissue organization and development [15]. The diameter of ECM components is approximately 1–500 nm, thus making electrospinning an advantageous technique, as it can be used to produce fibers throughout this range [16]. As the composition and structure of the ECM regulate the structure and biomechanical properties of the scaffold network, both the materials and fabrication methods should be carefully considered for the design of 3D scaffolds [17]. The human ECM is a 3D structure primarily composed of collagen, elastin, fibronectin, laminin, and several other natural polymers [18]. Therefore, it is often intuitive to exploit these polymers to fabricate 3D scaffolds for the design of target tissues and organs. Each tissue has an ECM with a unique biochemical composition and physical structure, and

accurately mimicking these features can regulate cellular spreading, motility, and lineage commitment [19, 20].

Although the relevant literature covers a wide range of uses of electrospinning, this review will focus on readily available and common fabrication methods and materials for the fabrication of 3D electrospun scaffolds for TE. We first summarized materials used for electrospinning and the merits of 3D nanofiber scaffolds over traditional 2D scaffolds. Subsequently, the latest trends in the fabrication forms and application of 3D electrospinning nanofiber scaffolds are presented. In addition, their individual effects are analyzed and compared to identify their advantages, limitations, and future outlooks (Table 1).

Materials Used for Electrospun Scaffolds Used in Tissue Engineering

One of the main advantages of electrospinning is its versatility of processing to create nanofiber scaffolds with multiple morphological and topological features. This processing flexibility allows the fabrication of 3D scaffolds from a wide range of materials, such as synthetic and natural polymers as well as their composites. These materials need to be biocompatible with the exogenous or endogenous cells as well as capable of performing or even enhancing the function of the native ECM without inducing undesirable toxic reactions to the surrounding tissues. Additionally, scaffolds need to exhibit appropriate biodegradation rate commensurate with the healing rate of tissues [21]. Typical scenarios include the application of scaffolds for osteochondral, musculoskeletal, cardiovascular, and nerve regeneration [22]. Polymers are central to the fabrication of scaffold materials owing to their tunable properties and help realize appropriate physical, biological and mechanical performance of resulting 3D scaffolds.

Natural polymers are considered as a preferred choice for electrospinning owing to their biocompatibility and biodegradability [22]. Besides, most of the natural polymers promote bioactivity due to the presence of cell-recognizable moieties. A wide range of natural polymers, such as chitosan [23], hyaluronic acid (HA) [24], silk fibroin (SF) [25], collagen (Col) [26], and gelatin (Gel) [27] are biocompatible and biodegradable, which have been extensively exploited for regenerative medicine and TE. Besides, decellularized extracellular matrix (dECM)-based electrospun scaffolds that mimic the complex biochemical properties and 3D structures of native mammalian ECM have received significant interest for tissue regeneration and clinical translation [28]. Most of the natural polymers can be directly used in electrospinning once they have been dissolved in an appropriate solvent [29]. Zhou et al. studied the effect of marine collagen due to its abundance and low price to understand and control the

mechanical behavior of collagen scaffolds [30]. It was found that marine collagen scaffolds could offer suitable tensile strength and thermal stability without inducing any obvious immune response during skin wound healing in rats [30]. Pang et al. reported that biodegradable chitosan scaffolds are biocompatible *in vitro* and *in vivo* [31]. Gurumurthy et al. [32] reinforced collagen matrix with elastin-like polypeptide (ELP) to improve mechanical properties. However, disadvantages of natural polymers include their inferior biomechanical properties, fast degradation *in vivo* and possible immunogenicity, which limit their clinical translation.

Alternatively, synthetic polymers, such as poly(vinyl alcohol) (PVA), poly(L-lactide) (PLLA), polycaprolactone (PCL), poly (glycolic acid) (PGA), poly(L-lactide-co- ϵ -caprolactone) (PLCL), and poly(lactic-co-glycolic acid) (PLGA) are also commonly used in electrospinning [33–36]. As compared to the natural polymers, the physicochemical properties of synthetic polymers can be easily tuned by appropriately selecting the content of monomers and initiators as well as by optimizing reaction conditions. Synthetic polymers are also easier to be tailored into various shapes and structures as needed for TE. However, despite these obvious advantages, synthetic polymers often lack cell affinity owing to the paucity of bioactive moieties, which largely limit their biomedical applications [37]. Electrospun scaffolds comprising natural and synthetic polymers could obviate these shortcomings. However, a mere combination of natural/synthetic polymers cannot satisfy all requirements of mimicking native ECM for TE. Natural ECM leverages a multitude of physicochemical and bioactive cues to the cells, which needs to be judiciously considered while choosing an appropriate material combination for electrospinning [38]. Typical examples include the fabrication of inorganic/organic hybrids comprising polymers and ceramics. Inorganic nanoparticles, such as nanohydroxyapatite (nHA), attapulgite, carbon nanotubes, and graphene have been widely exploited for the design of organic/inorganic hybrids [39]. Inorganic nanoparticles enhance the mechanical properties of the hybrids, which serve as an ideal platform for the long-term sustained release of drugs and TE applications [40]. Inorganic particles display a good loading capacity for bioactive molecules or drugs and have a variety of advantages in promoting cellular functions, especially in bone tissue engineering (BTE) [41–43]. Moreover, bioactive glasses also show great potential for application in BTE, which have been reported to contact with body fluids to form a hydroxycarbonate apatite (HCA) surface layer that releases soluble silica and calcium ions, thus stimulating bone progenitor cells to facilitate bone regeneration [44].

The selection of electrospun materials should be available for implantation and appropriately match the specific requirements of different individual medical applications. Given the complexity and a broad range of polymeric

biomaterials, efforts to optimize materials for application in research or clinical translation should focus on the development of novel materials with unique chemical compositions or tailored properties to fit the application. On the one hand, novel synthetic polymers with unique functions can be created to satisfy the demands of different applications. For example, Liang et al. [45] synthesized PCL-*grafted*-lignin copolymers by ring-opening polymerization and prepared nanofiber membranes via electrospinning for the treatment of osteoarthritis (OA). While PCL exhibits good mechanical properties, it is difficult to meet the specific requirements of OA therapy, both in terms of biocompatibility and bioactivity. Lignin, as a plant polyphenolic polymer, is known to effectively scavenge free radicals due to its phenolic hydroxyl groups [46]. However, lignin is brittle and of low viscosity, which renders its processability to be difficult for electrospinning [47]. Therefore, through polymerization reaction, a novel biomaterial with good mechanical properties, antioxidant properties and spinnability was obtained, which was subsequently electrospun and achieved satisfactory results in OA therapy. Alternatively, the hybrid scaffolds could be obtained by blending and co-spinning of materials to realize the complementary advantages of different components. Wang et al. [48] prepared hybrid SF/PLCL nanofibrous scaffolds for bone regeneration. The SF, a natural polymer displays good biocompatibility and anti-inflammatory properties, and has been shown to support mesenchymal stem cell (MSC) adhesion and osteogenesis as well as improve cell-scaffold interactions [49, 50]. The PLCL provides good mechanical support to ensure the structural integrity of scaffolds *in vivo* without a collapse. Consequently, the hybrid SF/PLCL scaffolds promoted trabecular bone regeneration as well as bone mineral density (BMD) in a cranial defect model in rats as compared to pure PLCL scaffolds. Similarly, the surface functionalization of nanofibrous scaffolds can be performed to further improve their properties. Sun et al. [51] prepared a polypyrrole (Ppy)-coated PLCL/SF nanofibrous nerve guidance conduit (NGC) to induce nerve regeneration. As the electrical stimulation has been reported to promote the regeneration of nerve tissues, these conductive scaffolds have great promise for TE [52]. Ppy has been shown to promote neurites outgrowth by leveraging electrical stimulation to the cells [53], while insolubility and brittleness restricts its processing via conventional electrospinning. Therefore, PLCL/SF NGC were immersed into a bath solution consisting of pyrrole (monomer), sodium para-toluene sulfonate (pTS, dopant) and FeCl₃ (an oxidizer) and realized Ppy-coated PLCL/SF NGC by polymerization. As compared to PLCL/SF NGC, Ppy-coated NGC exhibited better Schwann cells proliferation and remyelination.

Conclusively, the selection of the materials is pivotal to better mimic the physico-chemical and biological properties of the target tissues and organs.

Fabrication of 3D Electrospun Nanofiber Scaffolds and Their Biomedical Applications

The traditional electrospun scaffolds are dense 2D membranes, which possess limited thickness, low porosity, and poorly-interconnected pores. The small pore size distributed on the surface of nanofibrous membranes substantially hinders the infiltration of cells inside the entire scaffold, thus limiting their application in TE. In contrast, scaffolds constructed with a 3D nanofibrous network feature a microenvironment similar to *in vivo* settings for cell survival, allowing cells to proliferate and infiltrate conductively into scaffolds [54]. Variation in such morphological features influences cellular responses as well as regulates cell migration, differentiation, and matrix remodeling [55]. Therefore, in order to accurately mimic the *in vivo* microenvironment and induce tissue repair, it is imperative to fabricate 3D electrospun scaffolds.

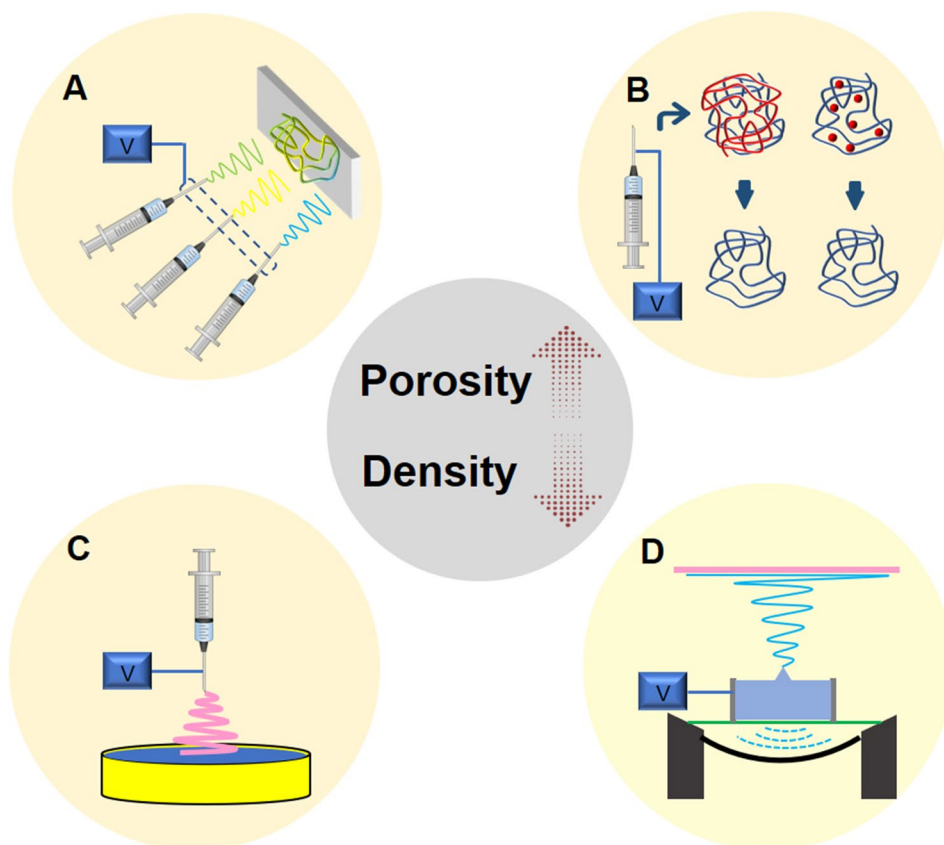
The fabrication of 3D scaffolds can be subdivided into two main sections, including (a) direct preparation and (b) post-processing of electrospun scaffolds. Of these, the direct

preparation methods display superiority in the timely fabrication of 3D porous scaffolds, which are mostly realized by varying the electrospinning parameters as well as by incorporating sacrificial agents. On the other hand, while post-processing methods offer an advantage in finely tuning the morphological as well as physicochemical properties, they require more complex procedures and special devices. Below, we first describe direct fabrication methods (Fig. 1), such as multilayering electrospinning, sacrificial agent electrospinning, wet electrospinning, and ultrasound-enhanced electrospinning. Thereafter, we enumerate post-processing strategies to realize 3D electrospun scaffolds.

Multilayering Electrospinning

Multilayered scaffolds are produced by collecting and stacking electrospun layers sequentially atop each other. Multilayered scaffolds may permit the fabrication of hybrid structures to better mimic the morphological and physicochemical features of tissues and organs. Wu et al. [56] designed a multilayered vascular scaffold manifesting a symmetrical structure using bi-directional electrospinning. Briefly, PLCL as well as collagen and chitosan were sequentially deposited to produce a layer-by-layer scaffold (Fig. 2A(i)). The final inner and outer layers of the obtained grafts were composed of collagen and chitosan, while the

Fig. 1 Schematic illustration of various methods to directly prepare 3D electrospun scaffolds and finely tune their morphological features, including multilayering electrospinning (A), sacrificial agent electrospinning (B), wet electrospinning (C), and ultrasound-enhanced electrospinning (D)



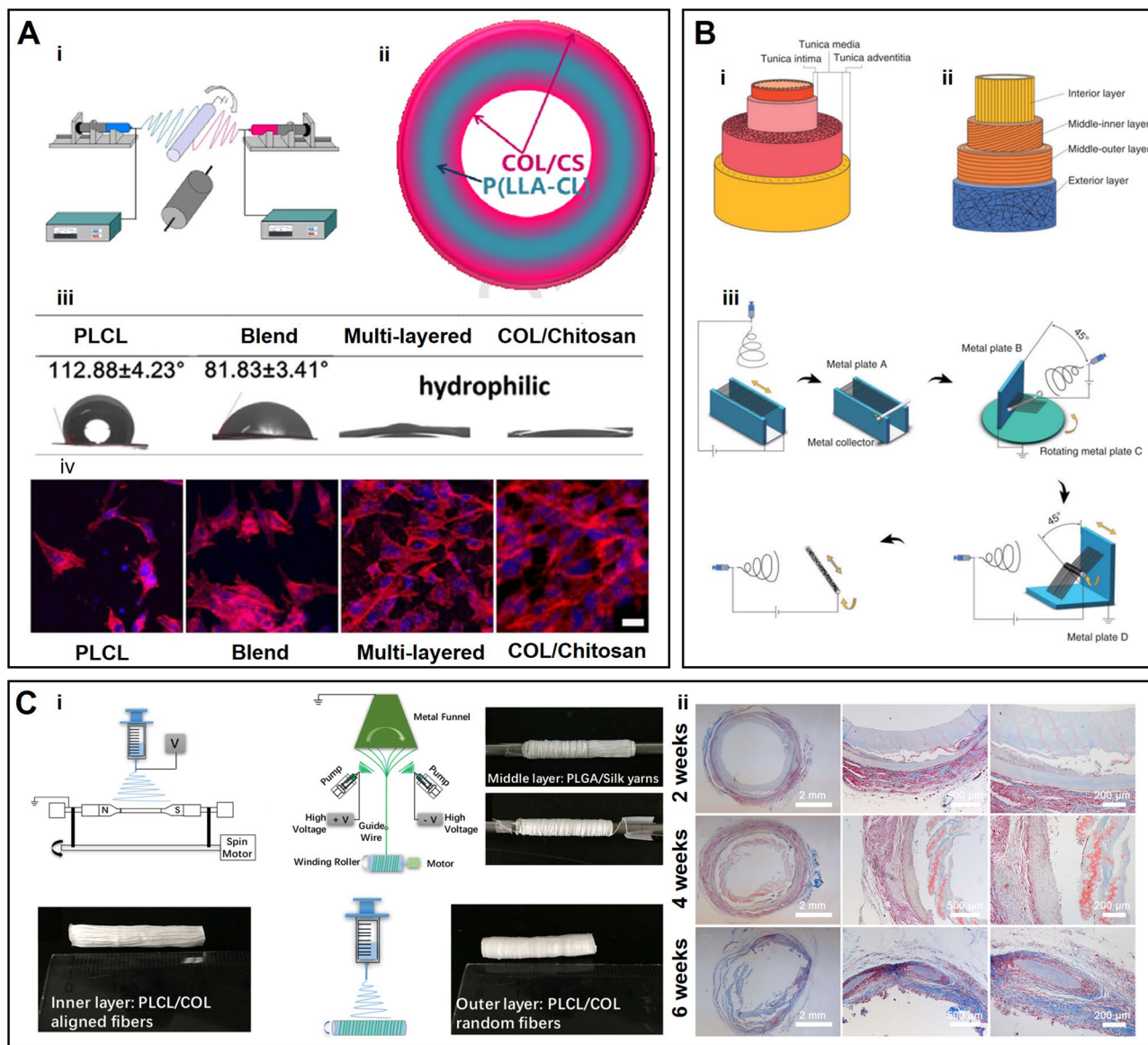


Fig. 2 **A** (i) Schematic representation of the bi-directional gradient electrospinning setup. (ii) Schematic structure of the cross section of the multilayered scaffold. (iii) Water contact angle of electrospun scaffolds. (iv) Confocal images of porcine iliac artery endothelial cells (PIECs) on different scaffolds after culturing for 3 days. **B** The schematic diagram of native blood vessel (i), small-diameter four-layered thermoplastic polyurethane tubular scaffold (ii) and the fabrication process of the tubular scaffold (iii). **C** (i) The schematic diagram showing the fabrication of tri-layer tubular graft. (ii) Masson's trichrome staining images of the transplanted grafts after subcutaneous embedding in mice. **A** (i–iv) Reproduced with permission [56]. Copyright 2015 Elsevier. **B** (i–iii) Reproduced with permission [57]. Copyright 2020 SAGE Publications. **C** (i, ii) Reproduced with permission [58]. Copyright 2018 Elsevier

intermediate layer was comprised of PLCL (Fig. 2A(ii)). PLCL was used to leverage a structural support to the grafts, while collagen and chitosan were exploited to promote the biocompatibility and improve cell-scaffolds interaction. The multilayered grafts exhibited higher hydrophilicity as well as facilitated the growth of porcine iliac artery endothelial cells (PIECs) than that of the PLCL scaffolds or those assembled by simple blending different components (Fig. 2A(iii, iv)). Similarly, Dias et al. [59] designed a multilayered nanofiber

scaffold exhibiting a 5-layered structure comprising of alternative layers of Gel and PCL (Gel/PCL/Gel/PCL/Gel). The PCL was used to promote structural stability, while Gel was exploited to promote the biocompatibility. Multilayered nanofiber scaffold displayed high porosity and good water permeability, and exhibited higher proportions of proliferating human dermal neonatal fibroblasts (hDNF) as evidenced by the higher numbers of Ki-67 positive cells, indicating their superiority for wound healing. The above design aims

to compositionally utilize multilayering electrospinning to achieve a layered distribution of synthetic and natural fibers and improve the host compatibility of the scaffold.

Multilayering electrospinning improves the affinity of the scaffold through alternate spinning of synthetic and natural materials, and is also able to fabricate scaffolds with multilayered biomimetic structures. Most of the human tissues display multilayered architecture distinctly differing in structural and morphological features. Blood vessels are composed of tunica intima, tunica media, and adventitia, each of which confers distinct functionality to the blood vessels. While the tunica intima is central to anti-coagulation and anti-thrombogenesis, tunica media and adventitia provide structural support and vasodilation for the smooth functioning of blood vessels (Fig. 2B(i)). Therefore, the development of vascular grafts with multiple layers, each with different morphology and function, is a current research priority. Hu et al. [57] prepared a four-layered thermoplastic polyurethane (TPU)/PCL/polyethylene glycol (PEG) tubular scaffold by multilayer electrospinning. The inner layer of the grafts was consisted of longitudinally-aligned nanofibers, the two intermediate layers were composed of circumferentially aligned fibers, while the outer layer was consisted of random fibers (Fig. 2B(ii)). Four devices were designed to prepare four types of fiber structures. The innermost layer was obtained by electrospinning the fibers on a copper wire. The second layer was obtained by tilting the collection device. The third layer was realized by using a rotating roller and finally the fourth layer was collected randomly (Fig. 2B(iii)). The resulting grafts exhibited excellent circumferential and longitudinal mechanical properties as well as improved adhesion and proliferation of human umbilical vein endothelial cell (HUVECs) than that of their random counterparts. Wu et al. [58] fabricated a tri-layered vascular graft manifesting structural and functional hierarchy. The inner layer was composed of PLCL/collagen aligned fibers, the middle layer of PLGA/SF yarn, and an outer layer of PLCL/collagen random fibers (Fig. 2C(i)). The outer layer of random fibers provided structural support to the entire tubular structure. The axially-aligned inner layer mimicked the endothelium morphology, while the middle layer regulated smooth muscle cells (SMCs) organization along with the single yarns. Subcutaneous implantation of grafts revealed host cell infiltration and ECM accumulation (Fig. 2C(ii)). This multilayered graft mimicking the native blood vessels may be beneficial for vascular remodeling.

Besides, several research groups have improved the functionality of multilayered electrospun scaffolds. Shokrollahi et al. [60] proposed the production of a three-layered scaffold consisting of PCL nanofibers as the first layer (hydrophobic layer), PCL and chamomile-loaded carboxyethyl chitosan (CECS)/PVA nanofibers as the middle layer (transition layer), and CECS/PVA nanofibers as the third layer

(hydrophilic layer). The incorporation of chamomile into scaffolds improved their mechanical, antioxidative and anti-bacterial properties. Multilayered electrospun scaffolds have also been exploited as controlled release systems. Birhanu et al. [61] created a multilayered scaffold loaded with dexamethasone in the middle layer, which afforded sustained drug release than that of the scaffolds containing the blended drug.

From the above cases, it is seen that multilayer electrospinning allow for the fabrication of scaffolds with well-defined morphology. By changing the composition, spinning parameters, or adding bioactive substances after a single spinning process, the biocompatibility and bioactivity of the scaffold are improved, but it fails to change the tight-stacked structure inside the scaffold, which requires more advanced design to solve.

Sacrificial agent electrospinning

Since electrospun scaffolds exhibit small pore size, which constricts host cell infiltration and remodeling, it is imperative to fabricate scaffolds displaying sufficient porosity and large pore size. Sacrificial electrospinning helps improve an overall porosity and pore size of scaffolds. By using sacrificial electrospinning, a sacrificial agent, which later can be eluted from the scaffolds, is spun along with the polymer. Sacrificial agents including polymers, such as poly(ethylene oxide) (PEO), PVA, polyvinylpyrrolidone (PVP), and gelatin as well as sodium chloride (NaCl) and sugar have been widely exploited [62, 65]. A fast-dissolving sacrificial agent and a slow degrading polymer are often blended to realize porous scaffolds. The sacrificial agent leaves behind voids, which increase the overall porosity of the scaffold. Besides, the pore size can be tailored by varying the size of the sacrificial agent. Aghajanpoor et al. [62] exploited water-soluble PEO to increase the pore size of the PCL/nHA scaffolds for bone regeneration. As shown in Fig. 3A(i), two syringes containing PCL/nHA and PEO were placed in parallel for co-electrospinning to obtain nanofiber scaffolds with different weight ratio of PCL/nHA and PEO. The scaffolds were subsequently immersed in water for 48 h to remove PEO and dried at room temperature. By varying the PEO content from 0 to 40%, scaffolds with a range of pore sizes were fabricated. The pore size of scaffolds increased with an increase in PEO content, and more human dermal fibroblasts (HDF) were infiltrated into scaffolds exhibiting high PEO content (Fig. 3A(ii–v)). The mechanical properties of the scaffold decreased with an increase in the PEO content; Young's modulus of PCL scaffold was decreased from 2.51 to 1.65 MPa with the addition of 40% PEO. PVP has also been widely used as a sacrificial component to improve the porosity of nanofiber scaffolds [66, 67]. Türker et al. [63] fabricated composite scaffolds by co-electrospinning PVP

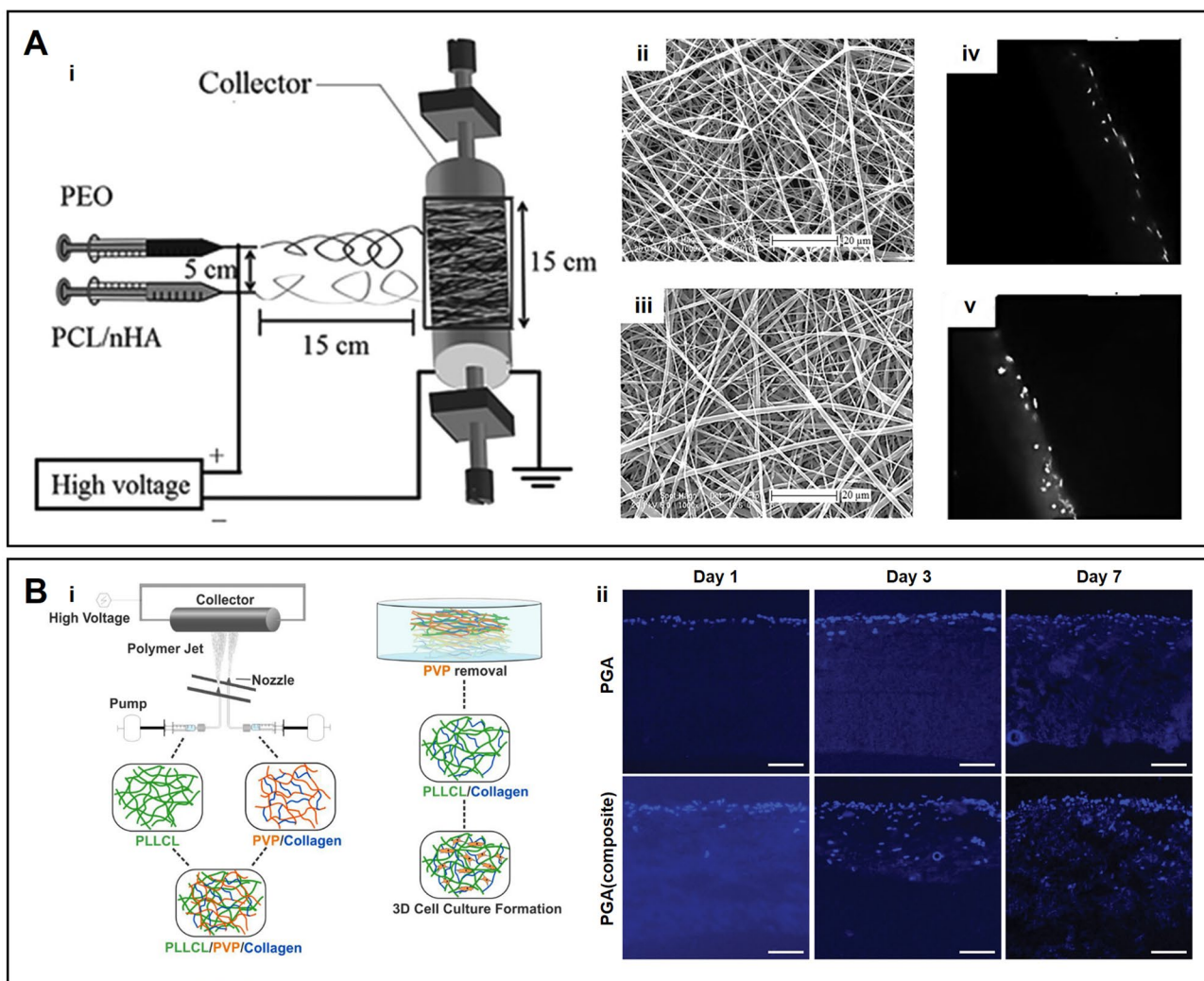


Fig. 3 **A** (i) Schematic of co-electrospinning setup for the preparation of dual-polymer composite. SEM images of the scaffolds prepared by co-electrospinning (ii) 100:0 and (iii) 70:30 weight ratios of PCL/nHA: PEO. Infiltration of human dermal fibroblasts (HDF) in the electrospun scaffolds after one week of culture for co-electrospinning (iv) 90:10 and (v) 80:20 weight ratios of PCL/nHA: PEO scaffolds. **B** (i) Schematic illustration of biomimetic PVP with PLCL and colla-

gen hybrid scaffold fabrication. (ii) DAPI staining revealing the infiltration of fibroblasts into the electrospun PGA and composite PGA scaffolds. Scale bars indicate 100 μm. **A** (i–v) Reproduced with permission [62]. Copyright 2017 Wiley. **B** (i) Reproduced with permission [63]. Copyright 2019 Elsevier. **B** (ii) Reproduced with permission [64]. Copyright 2019 Wiley

with PLCL and collagen, followed by the elution of PVP (Fig. 3B(i)). The removal of PVP fibers was ascertained based on the fiber diameter. The average fiber diameter was $0.349 \pm 0.07 \mu\text{m}$ for PVP and $1.55 \pm 0.27 \mu\text{m}$ for PLCL. After eluting PVP, the fiber diameter of the hybrid scaffold was maintained at $1.50 \pm 0.21 \mu\text{m}$. The resulting scaffolds with 3D networks promoted the adhesion and proliferation of NIH 3T3 mouse fibroblasts.

Alternatively, the introduction of sacrificial agents to scaffold can be introduced directly while electrospinning by sequential or concurrent electrospinning of sacrificial polymer part [68]. Hodge et al. [64] found comparable results by electrospinning PEO to increase the porosity of the most

commonly used biodegradable polymers, including PCL, PGA, and PLGA. Polymers and PEO were concurrently spun followed by the leaching of the latter. After PEO removal, scaffolds displayed a significant increase in the porosity compared to their counterparts devoid of electrospun PEO. The porosity of PGA scaffolds increased for up to 90% upon the removal of PEO; only PGA scaffolds showed a porosity value of 72%. DAPI staining further revealed an increase in the infiltration of cells after the leaching of PEO (300 μm) than that of PGA scaffolds (cell infiltration for up to 100 μm) (Fig. 3B(ii)).

The multilayered electrospinning described in the previous section failed to effectively solve the dense

arrangement of nanofibers, and the sacrificial agent electrospinning method seems to be more advantageous in this regard. Both the removal in the form of nanofibers or electrospayed nanoparticles results in a more porous structure for the scaffold.

Wet Electrospinning and Dynamic Liquid Electrospinning

Wet electrospinning utilizes the conventional electrospinning technique but modifies the collector into a grounded liquid bath to collect fibers (Fig. 4A (i)). While in a traditional

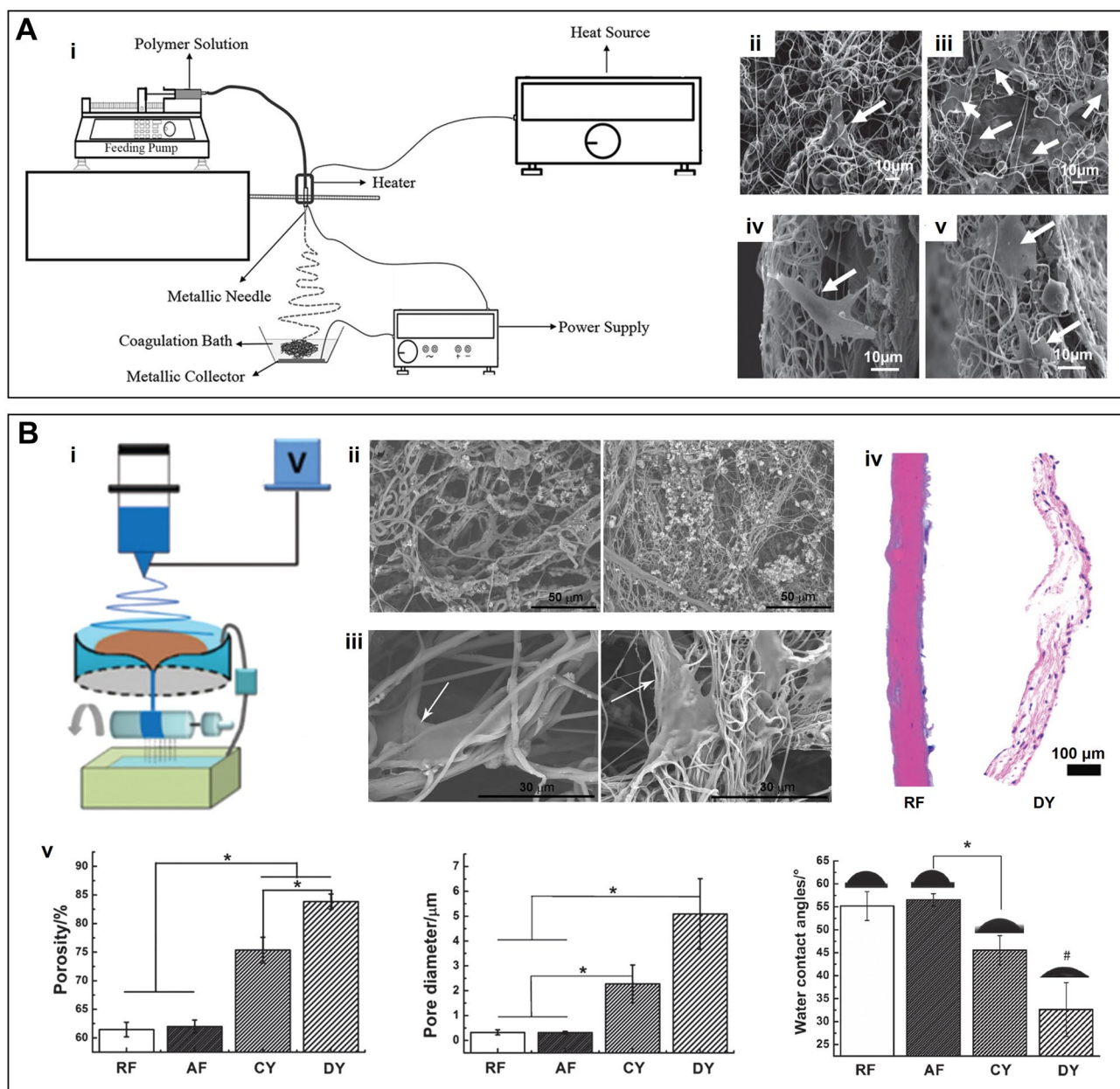


Fig. 4 **A** (i) Schematic diagram illustrating wet-electrospinning system. SEM images of cultured fibroblast cells on wet-electrospinning scaffold after 1 day (ii), 7 days (iii) culture and cross-sectional images after 5 days (iv) and 7 days (v). **B** (i) Schematic diagram of dynamic liquid electrospinning system. SEM micrographs of biomaterialized scaffolds (ii) and MC3T3-E1 cells on scaffolds (iii). (iv) H&E staining of the cross sections of random nanofibers (RF) and dynamic liquid electrospinning (DY) after culturing SMCs for 4 days. (v) Porosity,

ity, pore diameter and water contact angles of the RF, AF nanofibers and DY, CY nanofibers. **A** (i) Reproduced with permission [69]. Copyright 2016 Springer Nature. **A** (ii–v) Reproduced with permission [70]. Copyright 2017 Nihon Suisan Gakkai. **B** (i, iv, v) Reproduced with permission [71]. Copyright 2017 American Scientific Publishers. **B** (ii, iii) Reproduced with permission [72]. Copyright 2015 Springer Berlin Heidelberg

electrospinning setup, a solid collector is employed, wet electrospinning uses a liquid reservoir collector containing a wet medium. As soon as the nanofibers are collected, the wet medium can accumulate the space between the fibers and reduce the packing of fibers on top of each other. Moreover, a porogen can also be dispersed in the liquid bath to further increase the pore size of electrospun scaffolds.

Wet electrospinning commonly affords nanofiber membranes with high porosity as compared to normal electrospinning. Kishimoto et al. [70] electrospun SF using citric acid solution (pH 3.8) and *t*-butyl alcohol (*t*-BuOH) filled bath collector. The *t*-BuOH concentration significantly influenced the pore size and porosity of scaffolds, and when the concentration was 30%, the maximum pore size ($\approx 12 \mu\text{m}$) of scaffold was formed. The wet spun SF scaffolds displayed cells adhesion and proliferation both on the surface as well as the inner spaces of the 3D fibrous networks (Fig. 4A(ii–v)). Farzamfar et al. [73] prepared cellulose acetate/gelatin scaffold loaded with gabapentin in a water/ethanol bath collector by wet electrospinning. The resultant scaffolds displayed porosity value of 75.83%. These scaffolds improved the growth of Schwann cells as well as promoted sciatic nerve regeneration. These findings showed that neural tissue and skin tissue could be formed via 3D scaffolds produced from wet electrospinning.

With a minor modification, this wet electrospinning technique can be modified to dynamic liquid electrospinning to fabricate highly porous nano-yarn scaffolds (Fig. 4B(i)). A small central hole is added to the liquid bath at the bottom to create a vortex in the body of the liquid, where the collected fibers are drained through the small hole to be twisted and organized into a nano-yarn-like structure. This nano-yarn is then collected onto a rotating mandrel through the small hole to prepare fibrous scaffolds [74]. Wu et al. [75] also designed scaffolds by using dynamic liquid electrospinning, which improved the proliferation of pig iliac endothelial cells and MC3T3-E1 pre-osteoblastic cells. Besides, a capillary-like structure of cells was formed on the scaffold by day 7, suggesting that the use of nano-yarns can provide a template and promote the formation of capillary-like networks in vitro. Sun et al. [72] fabricated PLCL/SF nano-yarn scaffolds by dynamic liquid electrospinning. The nano-yarn scaffolds were immersed in calcium chloride (CaCl_2) and Disodium hydrogen phosphate (Na_2HPO_4) solutions for mineralization to promote the deposition of hydroxyapatite on the scaffolds and augment the osteo-conductivity of the scaffolds (Fig. 4B(ii)). As shown in Fig. 4B(iii), MC3T3-E1 cells were extended along the nanoyarn, and the porous structure of the scaffold provided sufficient space for cell growth and infiltration, indicating the good biocompatibility and potential of these scaffolds for bone tissue repair. Wu et al. [71] prepared PLCL/collagen nano-yarns by dynamic liquid electrospinning (DY), and compared them with random

nanofibers (RF), aligned nanofibers (AF), and conjugated nanoyarns (CY) in terms of physicochemical properties and biological evaluation. Of these scaffolds, the DY showed higher porosity, better hydrophilicity, and more SMCs infiltration than those of other groups (Fig. 4B(iv, v)), indicating the potential of DY for blood vessels regeneration.

Compared with the two methods introduced above, wet electrospinning has begun to modify the electrospun equipment to improve the porosity of the scaffold, especially the dynamic liquid electrospinning, which efficiently exploits the vortex generated by the water flow to twist nanofibers to prepare nano-yarn structure, is expected to be used for bio-related applications.

Ultrasound-Enhanced Electrospinning

While electrospinning is a simple and versatile process, its potential for fabricating nanofibers is somewhat restricted by the use of needles. Since during conventional electrospinning, the nozzle is often blocked, and the residual solvent in the nanofibers poses further hazards, ultrasound-enhanced electrospinning (USES) has been proposed, which can not only avoid the obstruction of nozzle but also promote the evaporation of solvent [76]. It is a needleless technique that focuses on high-frequency ultrasound bursts that generate a protrusion with a Taylor cone shape from the polymer solution (Fig. 5A(i)). When the polymer solution is charged with high voltage, a nanofiber stream is drawn from the protrusion to a grounded, solid collector (Fig. 5A(ii)) [77].

Nieminen et al. [76] first reported a USES technique that used ultrasound bursts to generate Taylor cones from the surface of a PEO polymer solution, which ejected nanofibers under a high voltage. The morphology of the nanofibers can be tuned by manipulating the ultrasonic parameters without using other chemical interventions. Figure 5B(i) showed SEM images of the nanofibers fabricated by USES at low, mid and high ultrasonic power. The nanofibers displayed only a few beads at low power, while much higher beads at high power. Besides, the nanofibers produced using high ultrasound were thinner compared to the fibers fabricated by using low or mid power (Fig. 5B(ii)); the mid power afforded narrow fiber diameter distribution (Fig. 5B(iii)). These results indicated that the nanofiber diameter can be modulated by varying the ultrasonic power without perturbing the chemical composition. Notably, the average diameter of the fibers prepared using the conventional electrospinning method was smaller than that of the fibers produced by using USES. This is attributable to the enhanced mass transfer resulted by the synergistic momentum induced by the electric field and ultrasonic power, which generated thick fibers.

Hakkarainen et al. [78] fabricated chitosan and PEO based nanofibrous scaffold encapsulating theophylline (TEO) using USES. Fiber diameter of scaffolds was tuned

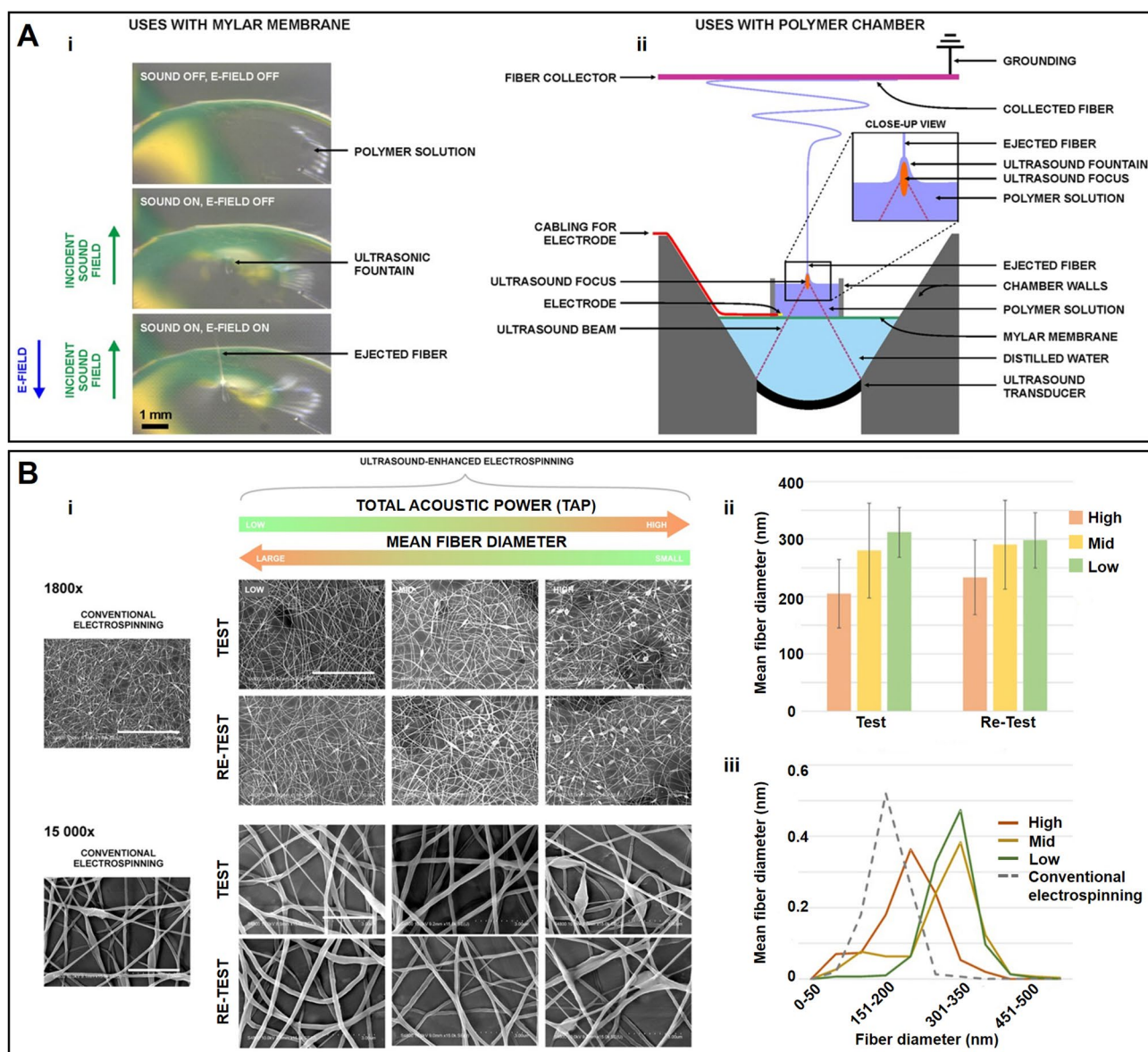


Fig. 5 **A** (i) Polymer droplets stimulated by ultrasound and electric field to generate liquid jets. (ii) Schematic illustration of the ultrasound-enhanced electrospinning (USES) system with a grounded target placed above the fountain to collect nanofibers. **B** SEM images

(i), diameter (ii) and diameter distribution (iii) of fibers produced with USES device at low, mid and high ultrasonic power. **A**, **B** Reproduced with permission [76]. Copyright 2018 Springer Nature

by changing ultrasonic parameters (i.e., frequency, pulse repetition frequency, and cycles per pulse). In agreement with Nieminen et al. [76], the diameter of USES-produced nanofibers was thicker than that of the traditional electrospun fibers. However, in biomedical applications, there is no intrinsic value in producing nanofibers as small as possible. For instance, in many TE scaffolds for wound repair, micron-sized fibers demonstrated superiority in cell adhesion and proliferation [79]. After a thorough characterization, including X-ray diffraction (XRD), differential scanning calorimetry (DSC), Fourier transform infrared (FTIR) spectroscopy,

the successful introduction of theophylline anhydrate was confirmed, demonstrating the potential application of USES in nanofibrous drug delivery systems. Similarly, Partheniadis et al. [80] fabricated nanofibers containing TEQ and PEO by USES. It was found that the nanofibers prepared by USES demonstrated higher Young's modulus in comparison to the fibers produced by using normal electrospinning, and drug release from nanofiber tablets was faster than that of the physically blended tablets.

From the above cases, the diameter of fibers obtained by USES is larger than that of conventional approach, but this

is not an obstacle to its development in the biomedical field, and USES is also a promising approach for the industrial production of nanofibers. However, USES is a multivariate process, and more research work is needed to elucidate its full potential and limitations for TE applications.

Electrospinning with Post-processing

Conventional electrospinning techniques afford nanofibrous membranes with 2D structures manifesting small pore size, which hinder cell infiltration and tissue formation. Besides, small pore size limits the transfer of nutrients and metabolic waste. Increasing the pore size of electrospun nanofibers thus holds great promise. Accordingly, a series of techniques, such as gas foaming, ultrasonication, short nanofibers assembly, electrospinning incorporated 3D printing, electrospraying, and various other methods, has been leveraged to produce 3D scaffolds from 2D membranes (Fig. 6). Since post-processing approaches mostly rely on electrospun nanofibers, they hardly require significant changes in the conventional electrospinning setup. Besides, post-processing approaches can also be combined with other fabrication techniques to improve the pore size, which will also be presented.

Electrospinning with Post-processing Gas Foaming

The gas-foaming technique is a simple and versatile post-processing technique to expand 2D nanofibrous membranes into 3D scaffolds and has been widely pursued in recent years. The mechanism of gas foaming is to trap gas bubbles

into nanofibers; the sudden escape of gas bubbles results into expanded scaffolds. Based on the mechanism of the production of gas bubbles, gas foaming techniques can be commonly classified into two types. The first one generates gas bubbles (e.g., hydrogen) via a chemical reaction and then exploits the nucleation and growth of gas bubbles in situ in the pores of nanofibers, thereby expanding the volume and porosity of the nanofiber membrane (Fig. 7A(i–v)) [81]. The second type involves placing a material, commonly polymeric along with a gas (e.g., carbon dioxide) in a chamber at an increasing pressure until the dissolution of the gas in the polymer. Once the pressure is relieved, large pores are formed thermodynamically [83]. This post-production method creates a highly-interconnected porous structure with a significant increase in the porosity and a multilayered structure and is advantageous for cell infiltration [82, 84].

To date, an array of techniques has been pursued to improve the gas foaming process to broaden its applicability to a wide range of materials, regardless of their hydrophilicity or hydrophobicity. Consequently, these manipulations have afforded a multitude of scaffolds with varying morphology and shape. Of these, gas-forming salts [e.g. sodium borohydride (NaBH_4)] are most commonly used in the gas-foaming process. In this post-treatment process, the space between the fibers is expanded by simply immersing the nanofiber membrane in a bath of gas salt to capture the gas bubbles. In one study, Joshi [85] et al. immersed hybrid nanofiber membranes comprising of PCL, nylon, cellulose, and polyvinylidene fluoride (PVDF) in NaBH_4 solution to fabricate sponge-like 3D scaffolds. These scaffolds exhibited larger pore size and higher porosity than that of their

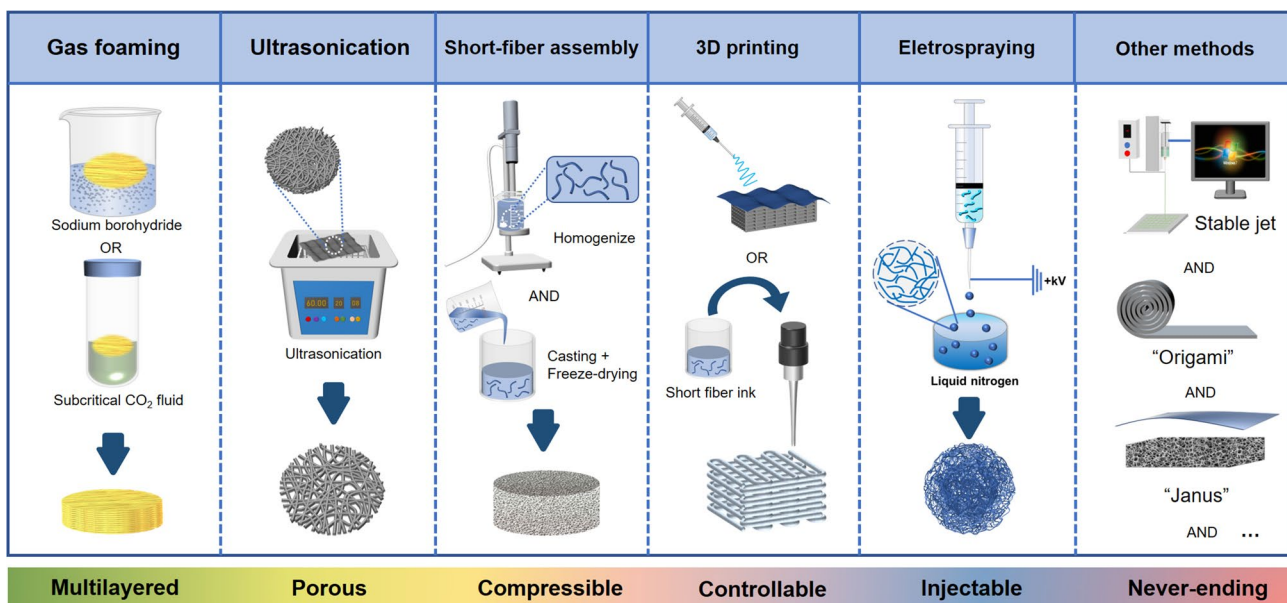


Fig. 6 Schematic diagram of the preparation of 3D electrospinning scaffolds based on post-processing methods

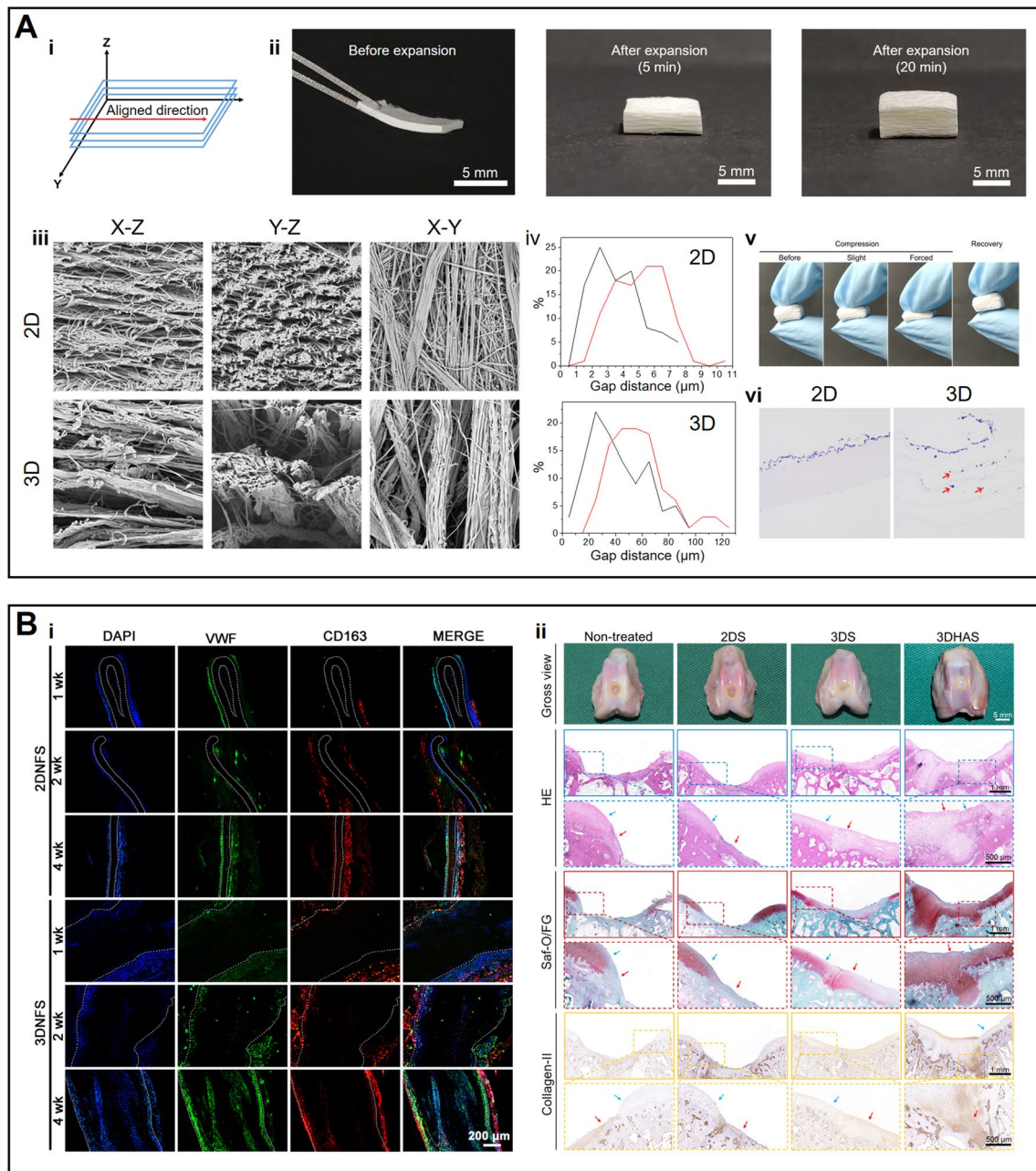


Fig. 7 **A** The expanded 3D nanofiber scaffold generated by gas-foaming technology. (i) The schematic shows the alignment direction of the scaffolds. (ii) Photographs of a raw nanofiber mat and expanded scaffold after foaming for up to 5 and 20 min, respectively. (iii) Morphology of scaffolds before and after expansion. (iv) Gap distances of raw mats and expanded scaffolds. (v) Mechanical properties of the gas foamed scaffolds. (vi) H&E staining of cell growth within raw mats and expanded scaffolds. **B** Representative applications of gas foamed scaffolds in tissue engineering. (i) Immunofluorescent stain-

ing for cell infiltration (DAPI), neovascularization (vWF), and macrophage (CD 163) markers of subcutaneous 2D implants (2DNFS) and 3D implants (3DNFS) in rats. (ii) Macroscopic, H&E, and Safranin-O/Fast Green staining images of the repaired cartilage defects in different groups (non-treated group, raw mat (2DS), expanded scaffold (3DS), and HA-crosslinked gas foamed scaffold (3DHAS) at 12 weeks after surgery. **A** (i–v), **B** (ii) Reproduced with permission [81]. Copyright 2021 Elsevier. **A** (vi), **B** (i) Reproduced with permission [82] Copyright 2021 Elsevier

2D counterparts. It was further revealed that the methanolic solution of NaBH_4 was more effective in expanding both polar and non-polar polymeric membranes, while the hydrolysis reaction was only suitable for polar polymers, which

may be attributed to the fast release of hydrogen gas resulted by the rapid decomposition of the methanolic solution. Jiang et al. [86] combined the gas-foaming technique with freeze-drying to obtain a 3D anisotropic PCL scaffold and a bilayer

tubular scaffold with a micron-sized lamellar structure and controlled gap width. In vitro assays demonstrated that the 3D scaffold could promote cell infiltration compared to as-spun 2D membranes; cells were mainly located only on the surface in the latter case. The thickness of the gas foamed scaffold was precisely controlled by using a custom mold. Subcutaneous implantation of 2D and 3D scaffolds in rats showed more cell infiltration and blood vessel formation as well as macrophages polarization toward M2 phenotypes in 3D scaffolds as compared to 2D scaffolds, which further validated the superiority of the gas-foamed scaffolds for tissue regeneration [87]. In addition, some ingenious designs for creating gas foamed scaffolds with different geometries have been proposed. Gao et al. [88] controlled the shape of 3D gas foamed scaffolds by mounting nanofibrous membranes in 3D printed molds of different shapes. 3D scaffolds of different shapes, including rings, bones, meniscus, and cartoon, were obtained, all of which exhibited good cytocompatibility. Besides, 2D electrospun PCL membranes have been expanded into 3D scaffolds after immersion in a CO₂-saturated ethanolic solution [89]. The 3D scaffold achieved for up to 95.3% porosity and fast cell proliferation. Jiang et al. [90] successfully expanded 2D membranes into 3D scaffolds by depressurizing subcritical CO₂ fluid, which was applicable to water-soluble polymers and preserved the bioactivity of the loaded drug as well as improved the biocompatibility.

The biomedical applications of gas foamed scaffolds have been a hotspot of research in recent years. Zhang et al. [91] applied a gas foamed scaffold composed of chitosan and PVA for wound healing. The sponge-like scaffold accelerated hemostasis and scar-less wound healing as well as promoted blood vessel formation. Gas foamed scaffolds were further exploited as fillers for NGC to promote peripheral nerve regeneration. Rao et al. [92] filled PLLA/SF based gas foamed sponge into a chitosan-based NGC and reported the higher proliferation of Schwann cells as well as better neurological functional recovery in conduits containing gas foamed scaffolds. In addition, gas foamed scaffolds were found to be appealing for cartilage TE. In a series of works, Chen et al. verified that the 3D PLCL/SF foamed scaffold promoted cell infiltration, neovascularization, and anti-inflammation after subcutaneous implantation (Fig. 7B(i)). Thereafter, HA cross-linked gas foamed scaffold (3DHAS) were shown to improve cartilage regeneration [81, 82]. Moreover, 3DHAS maintained the chondrocytes phenotypes, promoted more cartilage-specific ECM secretion, and achieved optimal repair in a rabbit joint defect model (Fig. 7B(ii)). Chen et al. [93] further prepared a size-tailored chondroitin sulfate (CS)-crosslinked gas foamed scaffold, and reported improved antioxidant activity and reduced production of inflammatory cytokines, such as interleukin (IL)-1 β and tumor necrosis factor (TNF)- α . These attempts

further broadened the avenues for improving the bioactivity of gas foamed scaffolds. Kim et al. [94] reported a modified gas foamed technique to fabricate a hierarchical scaffold with additional functions. Calcium hydroxide particles were deposited in situ on 3D scaffold fibers by the NaBH₄ reduction of calcium salt. Consequently, these 3D scaffolds not only improved the mechanical properties of the gas foamed scaffolds but also promoted cell infiltration, biomineralization, and osteogenesis, which are expected to further broaden the applicability of expanded scaffolds for bone tissue engineering applications.

Electrospinning with post-processing ultrasonication

Ultrasonication is a process for mechanical separation of electrospun nanofibers by applying ultrasound with an appropriate amplitude, intensity, and time. Ultrasonication reduces the packing density of the scaffolds by increasing the pore size and porosity, which may considerably improve cellular infiltration for TE (Fig. 8A(i)). Lee et al. [95] leveraged electrospinning and ultrasonication for the fabrication of a porous PLLA scaffold. As shown in Fig. 8A(ii), the thickness of the PLLA scaffolds increased after ultrasonication. The SEM images demonstrated that the ultrasonicated scaffolds were more porous as compared to the non-ultrasonic groups (Fig. 8A(iii)). In addition, the porosity of the scaffolds can be further increased by the ultrasonication time and energy, while the porosity was more dependent on the ultrasonic exposure time rather than on the energy (Fig. 8A(iv, v)). In vitro cell experiments showed that the ultrasonic group could increase the infiltration depth of fibroblasts compared with the non-ultrasonic group (Fig. 8A(vi)).

Ultrasonication is also often used with sacrificial method to further improve the porosity of the scaffold. This is because the ultrasonication process requires exposure to a liquid medium which provides a conducive environment for the removal of the sacrificial agent. Jeong et al. [96] prepared electrospun arginine-glycine-aspartic acid (RGD)-modified alginate nanofiber containing PEO and Pluronic F127 by varying the humidity, followed by ultrasonication to afford 3D scaffolds. Sodium alginate was chosen because it can be cross-linked by calcium ions, avoiding exposure to the toxic cross-linking agents. The nanofiber was further modified with RGD, aiming to regulate cell adhesion by providing integrin-binding sites. As expected, the membranes prepared at high humidity (HH) were significantly thicker (thickness, $438 \pm 68 \mu\text{m}$) than that of the membranes prepared at low humidity (LH) (thickness, $18 \pm 5 \mu\text{m}$); the former also displayed lower fibers' density and increased porosity. This is attributable to the fact that the high humidity simultaneously increases the charge density and fiber-fiber charge repulsion, resulting in thick scaffolds. After ultrasonication, the

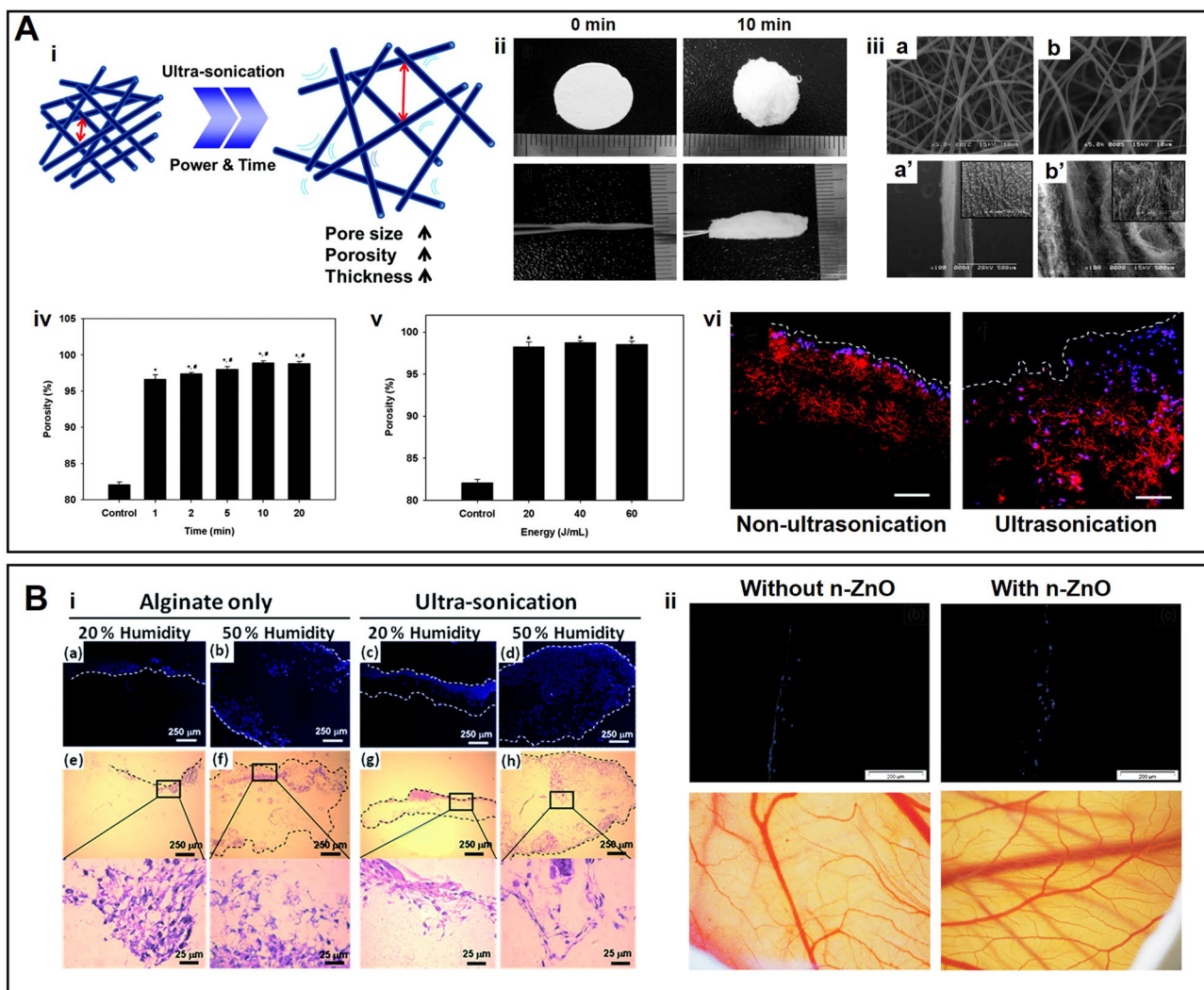


Fig. 8 **A** (i) Schematic illustration of 3D scaffold produced by the ultrasonication method. (ii) SEM images of non-ultrasonicated (a, a') and ultrasonicated PLLA scaffolds (b, b'). The average porosity of 3D scaffold by ultrasonication time (iv) and energy (v). (vi) Analysis of cellular infiltration in ultrasonicated and non-ultrasonicated scaffold. Bar 100 μ m. **(B)** (i) Fluorescence image of DAPI or H&E staining of HDF seeded alginate-only nanofibers and ultrasonicated nanofibers

fabricated at different humidity conditions. (ii) Evaluation of the cell infiltration and angiogenesis potential of the scaffolds with or without n-ZnO. **A** (i–v) Reproduced with permission [95]. Copyright 2011, Mary Ann Liebert. **B** (i) Reproduced with permission [96]. Copyright 2014 Royal Society of Chemistry. **B** (ii) Reproduced with permission [97] Copyright 2019 Wiley

cross-sectional thickness of the HH mats was increased from $515 \pm 24 \mu$ m to $1171 \pm 100 \mu$ m with an average pore size of 300μ m. In vitro cell experiments showed that both the high humidity environment and ultrasonication treatment promoted cell infiltration into the interior of scaffold owing to the higher porosity (Fig. 8B(i)). Similarly, Aghajanoor et al. [62] prepared nanofibrous scaffolds of PEO and PCL/nHA hybrids, PEO was removed by ultrasonication, which led to 1.9-fold increase in pore size as well as higher cellular infiltration, proliferation, and osteogenic differentiation of human mesenchymal stem cells. Rahmani et al. [97] fabricated nanofibrous scaffolds by co-electrospinning PEO and PCL (PCL/nHA/nZnO),

followed by ultrasonication. The nano-zinc oxide (nZnO) could generate reactive oxygen species (ROS) to improve the pro-angiogenic activity as well as promote bone regeneration through the release of Zn^{2+} [98, 99]. After ultrasonication, several secondary pores were detected, accompanied by an increase in the pore size of scaffolds, which significantly promoted cell infiltration in vitro. The ultrasound treated scaffolds promoted cell infiltration and angiogenesis as well as upregulated angiogenesis-related genes (Fig. 8B(ii)), which may have implications for bone tissue repair. Taken together, these data indicate that ultrasonication is an easy-to-perform post-processing method, which can afford the high porosity of scaffolds. Moreover,

ultrasonication can be combined with the other methods (e.g. sacrificial template method) to effectively improve the performance of 3D scaffolds.

Electrospinning with post-processing short-fiber assembly

As exceptional nanoscale building blocks for constructing 3D scaffolds, the homogenized electrospun short nanofibers are of great promise in regulating the physicochemical properties and mechanical flexibility of the scaffolds. Typically, nanofiber membranes are first cut into small pieces, followed by a homogeneous dispersion by using an ultrasonic homogenizer and freeze-drying to obtain 3D scaffolds (Fig. 9A(i–iii)) [100]. Different cross-linking strategies greatly influence the mechanical properties and biological functions of the scaffold. Cross-linking among short fibers can be accomplished by increasing the temperature while avoiding cross-linking agents. Mader et al. [103] fabricated PLLA or PLLA/PCL nanofibrous sponges by freeze-drying short nanofibers dispersions and thermal annealing mediated physical cross-linking among short nanofibers. 3D scaffolds showed good shape recovery and compressibility and promoted cell proliferation and infiltration. While, on the other hand, chemical cross-linking usually exploits functional groups on the fiber surface to form cross-linking agents-mediated covalent bond formation, thereby improving the integrity between fibers. Chen et al. [100] prepared 3D nanofiber scaffolds by freeze-drying electrospun gelatin/PLLA short nanofiber dispersion. Subsequently, the 3D scaffold was cross-linked by glutaraldehyde vapor and immersed in a glutamic acid solution to reduce the cytotoxicity. These superelastic gelatin/PLLA scaffolds also facilitated the proliferation of L-929 cells (Fig. 9A(iv–v)). Chen et al. [101] further optimized the cross-linking method of scaffolds and exploited thermal cross-linking to obtain structurally stable gelatin/PLLA 3D scaffolds as well as modified HA on 3D scaffolds to encourage cell recognition. The HA-modified 3D scaffolds exhibited better cartilage affinity and promoted cartilage repair in an articular cartilage defect model in rabbit (Fig. 9B(i, ii)). To further enhance the bioactivity of PLLA/gelatin 3D scaffolds, chondroitin sulfate was modified on the scaffolds. The chondroitin sulfate functionalized 3D scaffolds promoted the chondrogenic ability of bone mesenchymal stem cells (BMSCs) as well as upregulated the secretion of type II collagen and aggrecan. Besides, the modified scaffolds significantly reduced the expression of inflammatory factors while promoting cartilage tissue regeneration [104]. Thus, the cross-linking methods are chosen by taking into consideration the physicochemical properties of the material as well as by considering the effect of the crosslinking for tissue regeneration.

Cartilage-decellularized matrix (CDM) is expected to retain the major components and a variety of bioactive

cues, providing an ECM-like microenvironment for chondrification and cartilage regeneration [105, 106]. Li et al. [107] prepared a 3D composite scaffold composed of PCL/gelatin short fibers and CDM. While the short fiber network conferred excellent mechanical support to the scaffold, the CDM afforded the scaffold with bioactive functionalities to promote cartilage regeneration. The results showed that the composite scaffold could promote chondrocyte maturation and matrix secretion for cartilage repair in joint defects in rabbits. Shen et al. [108] fabricated a 3D scaffold consisting of PLGA electrospun short fibers, citrate-modified chitosan (CC), and CDM. The CC was introduced into the scaffolds to strengthen the mechanical properties and CDM was used to promote chondro-induction. The composite 3D scaffold promoted chondrocytes adhesion and proliferation as well as supported the secretion of cartilage-specific ECM glycosaminoglycans (GAGs) and in situ osteochondral regeneration in a rabbit defect model.

The interconnected macropores and hierarchical structure of 3D scaffolds facilitate bone repair. The osteoinductive properties of scaffolds can be further improved by leveraging osteogenic growth factors and bioactive glasses into the 3D networks. Ye et al. [102] prepared 3D scaffold comprising of nHA, PLLA, and gelatin short nanofibers and immobilized synthetic bone morphogenetic protein 2 (BMP-2)-derived peptide using polydopamine (pDA). The resulting scaffolds promoted the osteogenesis of BMSCs and bone regeneration in a cranial defect model in rats (Fig. 9B(iii–iv)). Wang et al. [109] designed a 3D elastic scaffold by freeze-drying the homogenized SiO₂-CaO bioactive glass nanofibers with chitosan serving as a crosslinker. This 3D scaffold displayed an elastic behavior with full recovery from 80% compression under wet state and promoted osteogenic differentiation of BMSCs as well as achieved vascularized bone regeneration in vivo.

Electrospinning with Post-processing Extrusion-Based 3D Printing

Additive manufacturing (AM), a modern technique for fabricating 3D scaffolds, improves the pore size and interconnectivity of scaffolds by amassing the materials in a layer-by-layer fashion. Being a simple and an economical technique, AM can be extended to a wide variety of materials for TE [114]. Despite these advantages, the large pore size of AM-based 3D scaffolds is not conducive to cell adhesion and infiltration. On the other hand, electrospun nanofibers provide an ECM-mimetic morphology as well as a large surface area for enhanced cell infiltration and tissue regeneration. Therefore, the convergence of 3D printing and electrospinning can allow the design of advanced scaffolds.

There are currently two main models for combining 3D printing with electrospinning to prepare 3D scaffolds.

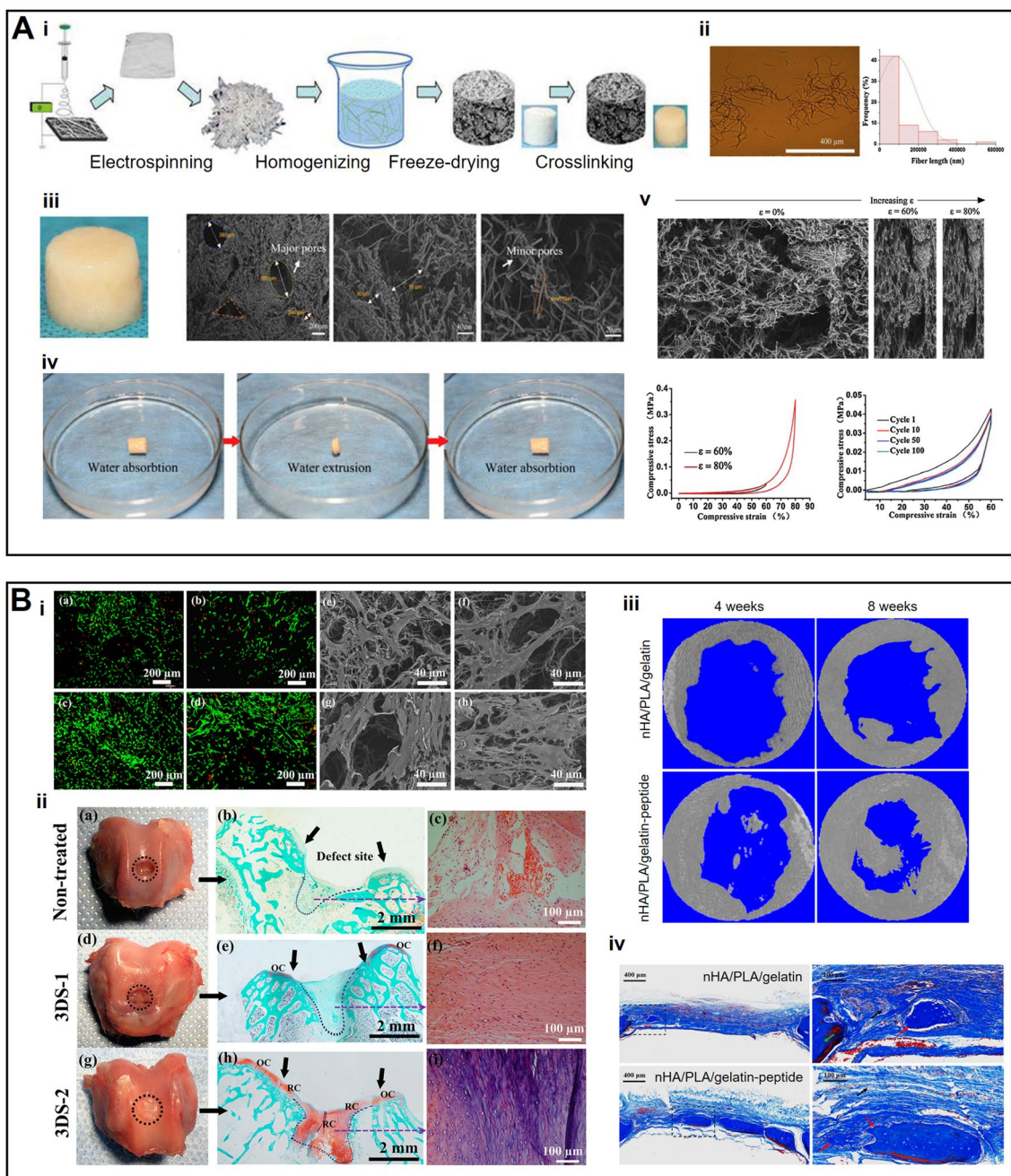


Fig. 9 A 3D nanofibrous scaffold afforded by short fiber assembly. (i) Schematic illustration of the process for the fabrication of 3D scaffold by short fibers self-assembly. (ii) Optical microscope image and fibers length distribution of the homogenized short nanofibers. SEM images (iii), water absorption (iv) and mechanical properties (v) of the 3D scaffolds. **B** Representative applications of 3D short fiber assembled scaffolds in TE. (i) Cell viability assay and cell morphology on 3D scaffolds. (ii) Macroscopic images and histological analy-

sis of the cartilage joints from three groups (non-treated groups, 3D PLLA/gelatin scaffolds (3DS-1), and 3D HA-modified PLLA/gelatin scaffolds (3DS-2)) at 12 weeks after surgery. (iii) Micro-CT images and Masson's trichrome stained images of rat cranial bones defects repaired by 3D scaffolds. A (i–v) Reproduced with permission [100]. Copyright 2016 Elsevier. B (i–ii) Reproduced with permission [101]. Copyright 2016 American Chemical Society. B (iii, iv) Reproduced with permission [102]. Copyright 2019 Elsevier

Amongst, the first one exploits 3D printing to precisely replicate a 3D structured scaffold with a specific size and design, and then leverages electrospinning to afford the deposition of nanofiber on the 3D printed networks

(Fig. 10A(i, ii)). For instance, Naghieh et al. [115] fabricated a porous PLLA/gelatin-forsterite scaffold utilizing extrusion-based cryogenic 3D printing. This commonly used and low-cost technique combines extrusion-based

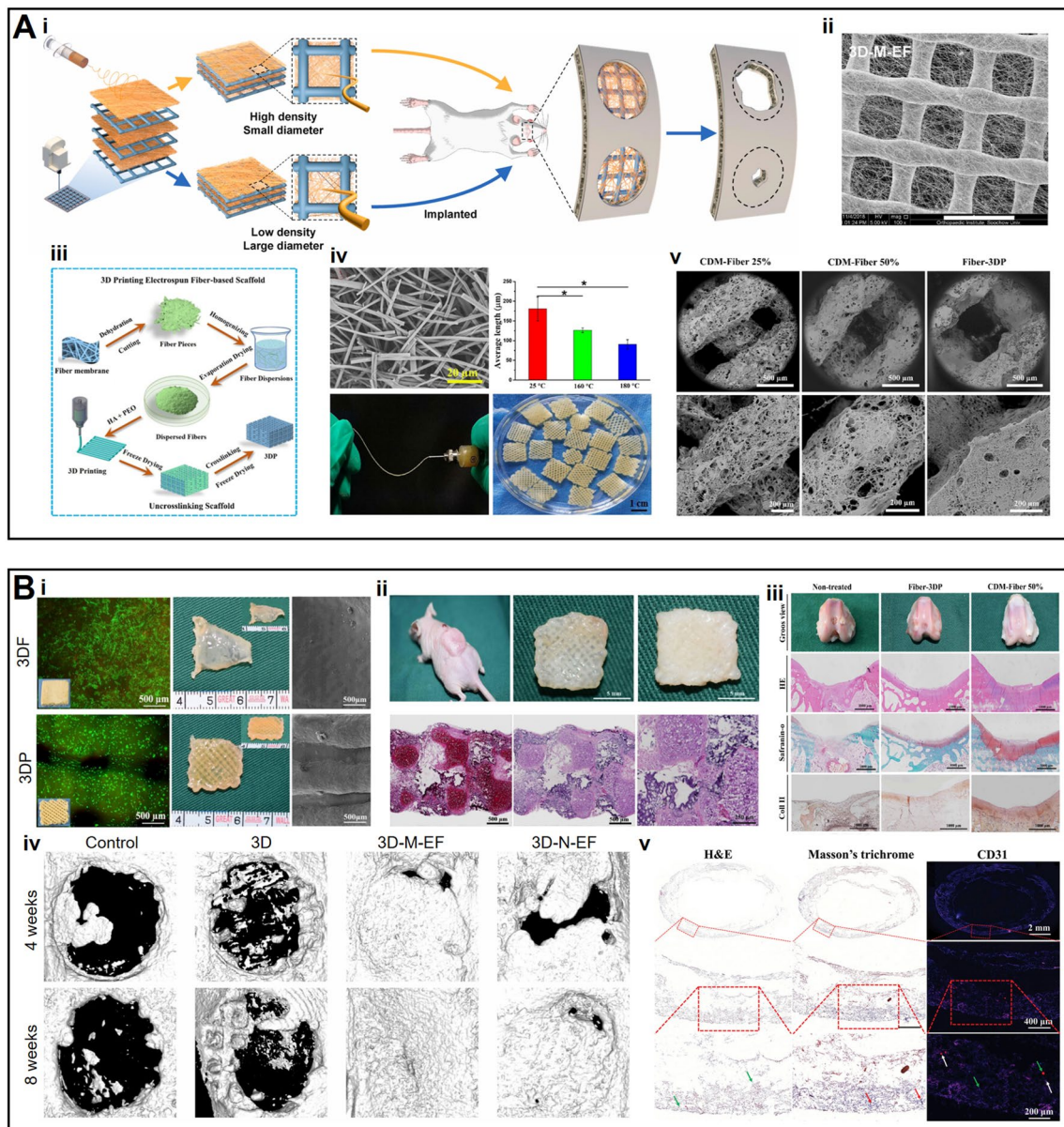


Fig. 10 A 3D scaffolds prepared by electrospinning-incorporated 3D printing approach. Schematic illustration (i) and morphology (ii) of the scaffolds fabricated by 3D printing and electrospinning. (iii) The fabrication steps of the 3D-printed fiber-based scaffold. (iv) SEM image, average lengths, injectability of electrospun dispersed fibers, and 3D-printed cuboid scaffolds. (v) SEM images of CDM-Fiber 25%, CDM-Fiber 50%, and Fiber-3DP. **B** Representative applications of electrospinning incorporated 3D printing scaffolds in TE. (i) Fluorescence photographs, gross appearance, and SEM images of chondrocytes seeded on the freeze-shaping scaffold (3DF) and 3D-printed scaffold (3DP). (ii) Gross view and histological analysis of regener-

ated cartilage in nude mice of Fiber-3DP group. (iii) Macroscopic images, histological and immunohistochemical analysis of the cartilage joints from Non-treated, Fiber-3DP, and CDM-Fiber 50% groups at 12 weeks after surgery. (iv) Micro-CT analysis of the bone repair capability of the scaffolds at the injury sites. (v) Histological and immunohistochemical analysis of tracheal biomimetic scaffolds after subcutaneous implantation. **A** (i, ii), **B** (iv) Reproduced with permission [110]. Copyright 2021 Elsevier. **A** (iii, v), **B** (i) Reproduced with permission [111]. Copyright 2019 Elsevier. **B** (iii, iv) Reproduced with permission [112]. Copyright 2020 Elsevier. **B** (v) Reproduced with permission [113]. Copyright 2021 Wiley

3D printing with traditional electrospinning to create scaffolds with high architectural complexity and mechanical support. The scaffolds had a porosity of 39% and showed the notable formation of bone-like apatite after its immersion in simulated body fluid solution. Similarly, Liu et al.

[110] prepared a composite scaffold combining electrospun PLLA fibers, and 3D printed PCL network, which promoted macrophages polarization to M2 phenotype as well as induced vascular regeneration and bone regeneration in a cranial defect model (Fig. 10B(iv)).

The second approach is to exploit electrospun short nanofiber-based bioinks for 3D printing. The 3D fibrous scaffold with pre-designed networks is then obtained after extruding the ink through a 3D drawing system. As the scaffolds are plotted, they are lyophilized and cross-linked to enhance inter-fiber connectivity and mechanical properties (Fig. 10A(iii)–(v)). Chen et al. [116] followed this general procedure to produce 3D printed electrospun fiber-based scaffolds for cartilage regeneration. In their study, they mixed 7% (w/v) HA solution 7% (w/v) PEO solution along with dry electrospun gelatin/PLGA fibrous powder to create the 3D printable ink. They found uniform cartilage regeneration well-integrated throughout the scaffold (Fig. 10B(i)). As compared to non-fibrous gelatin/PLGA scaffold, 3D printed fibrous scaffold exhibited better mechanical strength. Furthermore, for articular cartilage regeneration, Chen et al. exploited CDM-based bioink along with electrospun fibers to fabricate 3D-printed scaffolds with improved mechanical properties. The composite not only promoted cell adhesion and infiltration but also exhibited a good affinity for chondrocytes and good regeneration in a rabbit joint defect model (Fig. 10B(ii, iii)) [112]. Besides, Yuan et al. [113] exploited 3D printed frames to prepare tracheal scaffolds by converging 3D printing and electrospun short fibers. The 3D-printed framework provided good mechanical support

for the scaffold, while the short nanofibers afforded biomimetic morphology to provide more binding sites for the adhesion and growth of chondrocytes (Fig. 10B(v)).

Electrospinning with Post-processing Electrospaying

Injectable microspheres represent a new minimally invasive technique to deploy growth factors, drugs, cells or biologics, etc., for delivery to specific injury sites [42]. Unlike implantable scaffolds, injectable microspheres can be used to treat irregular defects through minimally invasive treatment without the need for invasive surgery [120]. While self-assembled and thermally induced phase separation (TIPS)-driven microspheres also inherit the above advantages, their applicability is limited and restricted to materials with specific groups on the surface [121]. Electrospinning incorporated electrospaying has been pursued in recent years as an alternative technique for preparing microspheres due to the versatility of electrospinning. Boda et al. [117] first reported the preparation of nanofiber microspheres by combining electrospinning with electrospaying. Nanofibers were chopped and homogenized at low temperature to form a homogeneous dispersion in water, and then the dispersion was electrospayed and received in liquid nitrogen to obtain nanofiber microspheres (Fig. 11A(i, ii)). This method

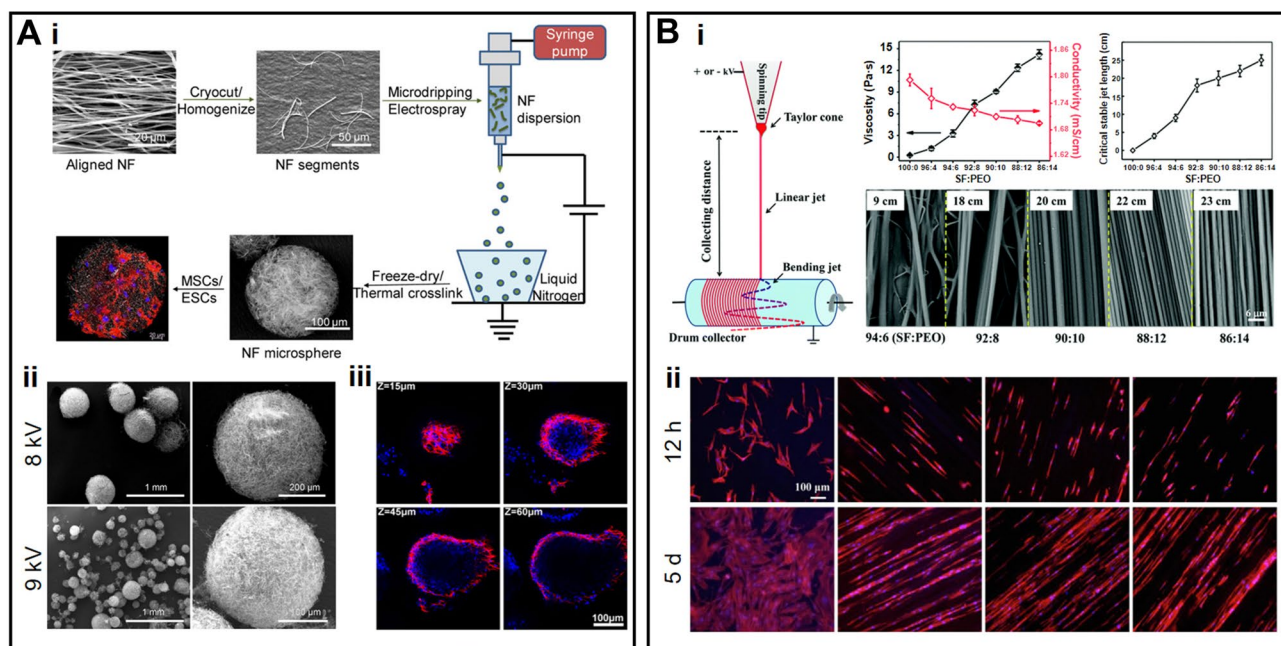


Fig. 11 **A** (i) Schematic overview of the fabrication of nanofiber microspheres. (ii) SEM image of the nanofiber microspheres fabricated with different voltage. (iii) Neural differentiation of mouse embryonic stem cells (mESCs) on nanofiber microspheres. **B** (i) Schematic diagram of the stabilized jet electrospinning process. Effects of PEO content on viscosity and conductivity of the SF/PEO solutions and critical stable jet lengths in stabilized jet electrospinning.

Morphologies of the aligned SF/PEO fibers collected at various critical stable jet lengths. (v) Fluorescence images of stained HDF on the aligned fiber scaffolds. **A** (i–iii) Reproduced with permission [117]. Copyright 2018 American Chemical Society. **B** (i) Reproduced with permission [118]. Copyright 2018, Royal Society of Chemistry. **B** (ii) Reproduced with permission [119]. Copyright 2019 Elsevier

Table 1 Methods of fabrication in 3D electrospinning scaffolds for tissue engineering

3D electrospinning method	Examples of materials used	Advantages	Disadvantages	References
Multilayering electrospinning	PLCL, PCL, TPU, PLGA, PEG, PVA, collagen, chitosan, gelatin	Simple set-up Thicker layer of aligned fiber deposition is possible Able to mix fibers of different materials of the desired ratio	Interference between the electrospinning jets Relatively dense structure	[56–61, 133]
Sacrificial agent electrospinning	PEO, PVA, PVP, PCL, PGA, PLGA, PLCL, nHA, silk fibroin, collagen, gelatin	Adjustable pore diameter and size Increased cell infiltration Uniform porous structure	Difficult to increase scaffold pore size Thicker fibrous scaffold is not possible	[62–68]
Wet electrospinning and dynamic liquid electrospinning	PLLA, PLCL, silk fibroin, gelatin, collagen, cellulose acetate,	Simple set-up Increased scaffold thickness, pore size Increased cell infiltration Thicker layer of aligned fiber deposition is possible	Difficult to scale up Thicker area of arrayed fiber assembly may not be possible Deposited fibers have to be dipped in water first before the yarn is formed Yarn collection speed is relatively slow	[70–75, 81, 134, 135]
Ultrasound-enhanced Electrospinning	PEO, chitosan, theophylline	Eliminate blockage of syringe and needle No clogging of solution at the source Possible to scale up	Set-up is complicated Variation of fiber diameter may be large	[76–78]
Gas foaming	PCL, PLCL, PVA, PLLA, nylon, PVDF, cellulose, chitosan, silk fibroin, HA, chondroitin sulfate	Increased porosity Increased cell infiltration Versatile without changing conventional electrospinning	Possibly reduced mechanical support Uneven pore sizes	[81, 82, 85–92] [93, 94]
Ultrasonication	PEO, PCL, PEA, alginate, chitosan, nHA,	Reduced scaffold density Increased porosity Simple formation procedure	Difficult to achieve the desired shape of the scaffold	[62, 95–97]
Short fiber assembly	PLLA, PCL, PLGA, gelatin, HA, chondroitin sulfate, CDM, chitosan, nHA, SiO ₂ -CaO	A decrease in scaffold packing density Versatile without changing conventional electrospinning Wide material versatility Increased thickness and porosity Controlled shape and size Shape memory and superabsorbent	Thicker fibrous scaffold is not possible Difficult to control microstructure	[100–109]
Extrusion-based 3D printing	PCL, PLLA, PLGA, PVA, PEO, gelatin, HA, CDM	Exact control of the structure of the scaffold Increased pore size Increased cell infiltration Suitable for scaled-up production	Fibers may not be aligned throughout the whole assembly Larger variation in the length of fibers Crosslinking agent toxicity Complex preparation process Various parameters need to be controlled Specific equipment	[110, 112–116]
Electrospraying	PCL, PLGA, PLLA, gelatin, GelMA, bioactive glass	Wide material versatility Injectable Controllable size	Complex preparation process Crosslinking agent toxicity Low yield	[117, 122–124]

Table 1 (continued)

3D electrospinning method	Examples of materials used	Advantages	Disadvantages	References
SJES, MEW and other combination methods	PEO, PCL, PLGA, chitosan, silk fibroin, decellularized WJ matrix (DWJM), gelatin	Able to control the direction of fiber alignment Patterning by fiber deposition is possible Improved cell infiltration speed and bioactivity	Thicker fibrous scaffold is not possible (for SJES and MEW) Complex preparation process (for other methods)	[118, 119, 125–132]

is widely applicable to a wide range of polymeric materials as well as inorganic bioactive glasses. Compared with solid microspheres, nanofiber microspheres have higher efficiency to be used as cell carriers and therefore are expected to be applied in cell therapy (Fig. 11A(ii)). John et al. [122] further improved the biofunction of nanofiber microspheres by tethering proteins and growth factors on the electro-sprayed nanofiber microspheres. Microspheres modified with BMP-2 promoted osteogenic differentiation of BMSCs, while vascular endothelial growth factor (VEGF) modified microspheres upregulated the vascular-specific proteins in HUVECs. These strategies further broaden the potential of electro-spray microspheres in developing biomimetic and injectable cell carriers. Zhang et al. [123] fabricated multifunctional PLGA-based microspheres by electro-spraying and modified them with gadolinium (Gd^{3+}) chelates and HA, followed by mixing with doxorubicin (DOX). These multifunctional drug-loaded nanofiber microspheres can achieve long-term release of DOX, reduce cancer cell metastasis, and render magnetic resonance (MR) imaging of tumors during the treatment, which may represent a good formulation strategy for local tumor chemotherapy. John et al. [124] further modified the approach for electro-spraying nanofiber microspheres. Porous nanofiber microspheres were prepared by bubble-mediated coaxial electro-spraying. Compared with nonporous nanofiber microspheres, open porous microspheres showed faster cell infiltration and host tissue integration, which may hold great potential for cell and drug delivery.

Other Methods

Stabilized jet electrospinning (SJES) was proposed as a solution to eliminate the whipping motion of the electrospinning jet. It involves using ultra-high molecular weight polymer, such as PEO, to modulate the viscoelasticity of the spinning solution, thereby affording a long yet stable jet during the spinning process and allowing the collection of well-aligned unidirectional fiber arrays [125]. Yi et al. [118] fabricated SF-based fibrous scaffold with anisotropic structures using SJES. With the addition of PEO as the fiber-forming component, highly aligned and high-strength SF fibers were obtained (Fig. 11B(i)), which supported the adhesion, migration, and growth of induced pluripotent stem cell-derived mesenchymal stem cells (iPSC-MSCs) along the fiber axis. Shen et al. [119] prepared unidirectional core/shell type chitosan/PLGA nanofibers by using coaxial electrospinning modified SJES method. These scaffolds were designed to address the aseptic inflammation caused by the degradation of aliphatic polyesters for TE applications. In vitro experiments showed that chitosan-mediated fibers supported an elongated cell shape with preferential orientation along the fiber axis (Fig. 11B(ii)) as well as significantly reduced

the secretion of inflammatory factors *in vitro*, and down-regulated the expression of relevant inflammatory genes in a simulated acidic environment. In addition, subcutaneous implantation of nanofibers demonstrated their potential for the recruitment of inflammatory cells and the formation of foreign body giant cells.

As an improvement of the SJES technique, the ‘electro-writing’ technique has been developed, which follows a computer-controlled predesigned moving path of the needle tip resulting in the management of pore size, shape, and thickness of the scaffolds [126]. Melt electro-writing (MEW), as one of the representative techniques of electro-writing, has been widely exploited in the field of TE [127]. The material is first melted and then extruded, and an electrostatic field is applied to stretch the extruded coarse fibers with a maximum precision of 1 μm . The printed fibers are stacked in a layer-by-layer manner following the moving paths regulated by a computer. Han et al. [128] prepared gelatin/PLGA-based composite scaffolds containing transforming growth factor- β 1 (TGF- β 1)-loaded PLGA microspheres using MEW. To obtain this composite structure, microspheres containing cytokines were sprayed onto the scaffold after printing every ten layers of the networks. This study optimized the viscosity of the ink in the MEW processing and suggested that 20–30 Pa s may be an appropriate value of the viscosity, and also found that the TGF- β -loaded composite could promote the cartilage differentiation of BMSCs, with the best repair outcome in a rabbit cartilage defect model. Similarly, Han et al. [129] employed MEW to manufacture a PCL-based composite scaffold containing cytokine-loaded microspheres, including morphogenetic protein-7 (BMP-7) and insulin-like growth factor-1 (IGF-1). BMP-7 (promoting chondrocyte secretion of proteoglycan 4) was loaded in the superficial layer of the composite scaffold, IGF-1 (enhancing the production of type II collagen and aggrecan) was located in the middle layer, and HA (promoting chondrocyte differentiation to deep cartilage) was located in the bottom layer. This design of environmental differences between scaffold layers contributed to the regional heterogeneity of chondrocyte secretory proteins, achieving excellent repair results in rabbit cartilage defect models.

Other approaches adopt a more complex methodology, combining various post-processing methods to improve the physicochemical properties and bioactivity of the scaffold. Xu et al. [130] rolled chondrocyte-membrane construct around a silicon tube to construct a 3D trachea-shaped scaffold with a controllable lumen diameter and wall thickness, which achieved encouraging repair outcome in a segmental tracheal lesion rabbit model. John et al. [131] introduced a method to prepare 3D scaffolds with patterned macrochannels by using 3D printed scaffolds as sacrificial templates combined with short fibers. Compared with the scaffolds lacking macrochannels, 3D macroporous scaffolds showed

enhanced cell infiltration and better host tissue integration, and this novel class of nanofiber fabrication approach further improved the short-fiber casting technique for rapid cellular infiltration. Zhang et al. [132] prepared a Janus nanofibrous aerogel for diabetic wound healing. A 3D nanofiber scaffold composed of quaternized chitosan/PVA (QCS/PVA) homogeneous nanofibers was obtained by freeze casting, and then curcumin /PCL nanofibers were further electrospun on their surface. The Janus 3D aerogel achieved autonomous and rapid delivery of exudate and exhibited good antibacterial and antioxidant properties to synergistically shorten the inflammation phase and promote diabetic wound healing.

Conclusions and Future Outlooks

Conclusively, a series of approaches has been put forward to afford electrospun 3D scaffolds to promote cell infiltration and neo-tissue formation, which results into the large pore size and high porosity. While conventional electrospinning affords 2D nanofibrous membranes with high packing density along with small pore size and porosity, advanced fabrication techniques help realize the production of 3D scaffolds exhibiting superior porosity, pore size, pore interconnectivity, and surface-to-volume ratio. This improvement in the physicochemical properties of scaffolds may not only beneficial for cell orchestration but also for improving cell-cell and cell-ECM cross-talk as well as the diffusion and transport of nutrients and oxygen for tissue survival *in vitro* and integration into host tissues/organs *in vivo*. While advanced fabrication techniques, including multilayered electrospinning, sacrificial template method, and wet electrospinning, which are the derivative technologies of conventional electrospinning and mainly rely on the accumulation of fiber layers, they are insufficient for improving the porosity and pore size of 3D scaffolds. Similarly, although these techniques permit the fabrication of improved scaffolds as compared to the conventional electrospinning method, the poor control over the precise regulation of microstructure and the distribution of micropores hamper their applicability. Alternatively, post-processing methods are inexpensive and afford a precise control over the microstructure of 3D scaffolds. However, these methods also have inherent limitations associated with them.

First, while gas foaming methods afford 3D scaffolds with high porosity and pore size compared with the 2D nanofibrous membranes, they adversely affect the structural integrity and mechanical stability of scaffolds [82]. Similarly, short-fiber based self-assembly method requires additional cross-linking and processing molds. Besides, short fiber self-assembly based method is tedious to be exploited for flexible and elastic materials, which cannot form uniform short-fiber dispersions. The approaches associated with 3D printing are

constricted by the requirements of the special instrumentation. Additional techniques such as ultrasound-enhanced electrospinning have yet not been developed and applied in a well-established manner. Moreover, specialized designs for sophisticated biomedical applications are still scarce, and more investments and trials are warranted for their eventual clinical translation.

Second, due to the unique morphological and mechanical properties of different tissues, future research should focus on the precise engineering of 3D scaffolds that can be adapted to the host tissues and organs. For cartilage tissue regeneration, scaffolds require sufficient elasticity to withstand compression and deformation of osteochondral tissues. Consequently, different types of crosslinking approaches have been introduced to afford elastic 3D scaffolds. The cross-linked network maintains the structural stability of the scaffold under compression as well as improves the water absorption capacity. Tendon and ligament tissues necessitate scaffolds with anisotropic mechanical properties, for which aligned micro/nanofibrous structures have been designed. While 3D scaffolds possess high porosity, they lack mechanical properties commensurate with the targeted tissues and organs and therefore need further optimization. On one hand, this issue can be addressed by delicate post-treatment and modification, such as *in situ* biomineralization, random layer strengthening, chemical cross-linking, etc. Therefore, further research is required to overcome the limitations associated with the current approaches to realize 3D scaffolds with tissue or organ matching mechanical properties.

Third, while the aforementioned methods mainly emphasize on the structural modification of the scaffold, more efforts are needed to improve the bioactivity of 3D scaffolds. Cell infiltration into scaffolds can be improved by incorporating bioactive cues. *In vivo*, cells perceive an array of biochemical cues, such as soluble signals and ECM-immobilized growth factors, biomimicking these features into 3D scaffolds may further enhance their applicability for TE. Cytokines and chemokines have been reported to induce cell egress and chemotaxis. Besides, GAGs foster sequestration of exogenous and endogenous growth factors, which may be amenable for designing advanced 3D scaffolds [136]. Likewise, platelet-rich plasma (PRP) can also be incorporated into electrospun nanofibers to improve the chemotaxis of cells and foster cell infiltration [137]. Other types of bioactive growth factors, such as BMP-2 and VEGF can promote osteogenesis and angiogenesis, which may be conducive for bone regeneration [102, 138]. Owing to the porous structure of the 3D scaffold, problems such as the poor distribution of bioactive molecules and initial rapid release need to be carefully considered.

Fourth, 3D scaffolds could mimic the hierarchical architecture of ECM. *In silico* studies focused to predict

the final pore size, porosity, surface roughness, and other properties of the scaffolds under different parameters may provide an indispensable information for an intelligent design of 3D scaffolds [139].

Fifth, as most polymers exploited for electrospinning are water insoluble, the use of highly toxic organic solvents is inevitable. Frequently used solvents, including dimethylformamide, dichloromethane, tetrahydrofuran, hexafluoroisopropanol, chloroform, etc., are highly toxic. The residual solvents on the fibers may have a negative effect on the biosafety of the scaffolds [140]. While it has been reported that most of the low boiling solvents can be removed by vacuum and heat treatment [141], considering environmental friendliness and biocompatibility issues, the use of the non-toxic solvents may hold great promise to for the further advancing of electrospun scaffolds for TE. Lastly, the issues related to scaling up, fine-tuning of properties, and cost competitiveness for achieving customized scaffolds with tissue-specific properties and material components in appropriate proportions remain to be solved.

Acknowledgements The authors would like to thank the financial support from National Nature Science Foundation of China (No. 32050410286), Science and Technology Commission of Shanghai Municipality (No. 20S31900900, 20DZ2254900), and Sino German Science Foundation Research Exchange Center (M-0263), National Advanced Functional Fiber Innovation Center (2021-fx020301), International Cooperation of 2021–2022 China and Poland Science and Technology Personnel Exchange Program (No. 17).

Declarations

Conflict of interest The authors declare no conflicts of interest.

References

1. Dvir T, Timko BP, Kohane DS, Langer R. Nanotechnological strategies for engineering complex tissues. *Nat Nanotechnol* **2011**;6:13–22. <https://doi.org/10.1038/nnano.2010.246>.
2. Cheng J, Jun Y, Qin J, Lee SH. Electrospinning versus microfluidic spinning of functional fibers for biomedical applications. *Biomaterials* **2017**;114:121–43. <https://doi.org/10.1016/j.biomaterials.2016.10.040>.
3. Wan X, Zhao Y, Li Z, Li L. Emerging polymeric electrospun fibers: from structural diversity to application in flexible bioelectronics and tissue engineering. *Exploration* **2022**;2:20210029. <https://doi.org/10.1002/exp.20210029>.
4. Matson JB, Zha RH, Stupp SI. Peptide self-assembly for crafting functional biological materials. *Curr Opin Solid State Mater Sci* **2011**;15:225–35. <https://doi.org/10.1016/j.cossms.2011.08.001>.
5. Holzwarth JM, Ma PX. Biomimetic nanofibrous scaffolds for bone tissue engineering. *Biomaterials* **2011**;32:9622–9. <https://doi.org/10.1016/j.biomaterials.2011.09.009>.
6. Wade RJ, Burdick JA. Engineering ECM signals into biomaterials. *Mater Today* **2012**;15:454–9. [https://doi.org/10.1016/S1369-7021\(12\)70197-9](https://doi.org/10.1016/S1369-7021(12)70197-9).

7. Khajavi R, Abbasipour M, Bahador A. Electrospun biodegradable nanofibers scaffolds for bone tissue engineering. *J Appl Polym Sci* **2016**;133:1–19. <https://doi.org/10.1002/app.42883> .
8. Greiner A, Wendorff JH. Electrospinning: a fascinating method for the preparation of ultrathin fibers. *Angew Chem Int Ed* **2007**;46:5670–703. <https://doi.org/10.1002/anie.200604646> .
9. Wang X, Ding B, Li B. Biomimetic electrospun nanofibrous structures for tissue engineering. *Mater Today* **2013**;16:229–41. <https://doi.org/10.1016/j.mattod.2013.06.005> .
10. Li D, Xia Y. Electrospinning of nanofibers: Reinventing the wheel? *Adv Mater* **2004**;16:1151–70. <https://doi.org/10.1002/adma.200400719> .
11. Abd Razak SI, Wahab IF, Fadil F, Dahli FN, Md Khudzari AZ, Adeli H. A review of electrospun conductive polyaniline based nanofiber composites and blends: processing features, applications, and future directions. *Adv Mater Sci Eng*. **2015**. <https://doi.org/10.1155/2015/356286>.
12. Xue J, Xie J, Liu W, Xia Y. Electrospun nanofibers: new concepts, materials, and applications. *Acc Chem Res* **2017**;50:1976–87. <https://doi.org/10.1021/acs.accounts.7b00218> .
13. Chen Y, Sha M, Liu M, Morsi Y, Mo X. Advanced fabrication for electrospun three-dimensional nanofiber aerogels and scaffolds. *Bioact Mater* **2020**;5:963–79. <https://doi.org/10.1016/j.bioactmat.2020.06.023> .
14. Liu W, Thomopoulos S, Xia Y. Electrospun nanofibers for regenerative medicine. *Adv Healthc Mater* **2012**;1:10–25. <https://doi.org/10.1002/adhm.201100021> .
15. Frantz C, Stewart KM, Weaver VM. The extracellular matrix at a glance. *J Cell Sci* **2010**;123:4195–200. <https://doi.org/10.1242/jcs.023820> .
16. Bancelin S, Aimé C, Gusachenko I, Kowalczyk L, Latour G, Coradin T, Schanne-Klein MC. Determination of collagen fibril size via absolute measurements of second-harmonic generation signals. *Nat Commun* **2014**;5:1–8. <https://doi.org/10.1038/ncomms5920> .
17. Agarwal S, Wendorff JH, Greiner A. Progress in the field of electrospinning for tissue engineering applications. *Adv Mater* **2009**;21:3343–51. <https://doi.org/10.1002/adma.200803092> .
18. Aamodt JM, Grainger DW. Extracellular matrix-based biomaterial scaffolds and the host response. *Biomaterials* **2016**;86:68–82. <https://doi.org/10.1016/j.biomaterials.2016.02.003> .
19. Du J, Yarema KJ. Carbohydrate engineered cells for regenerative medicine. *Adv Drug Deliv Rev* **2010**;62:671–82. <https://doi.org/10.1016/j.addr.2010.01.003> .
20. Xie X, Chen Y, Wang X, Xu X, Shen Y, Aldalbahi A, Fetzi AE, Bowlin GL, El-Newehy M, Mo X. Electrospinning nanofiber scaffolds for soft and hard tissue regeneration. *J Mater Sci Technol*. **2020**;59:243–61. <https://doi.org/10.1016/j.jmst.2020.04.037>.
21. Dutta RC, Dey M, Dutta AK, Basu B. Competent processing techniques for scaffolds in tissue engineering. *Biotechnol Adv* **2017**;35:240–50. <https://doi.org/10.1016/j.biotechadv.2017.01.001> .
22. Tang X, Thankappan SK, Lee P, Fard SE, Harmon MD, Tran K, Yu X. Polymeric biomaterials in tissue engineering and regenerative medicine. Elsevier Inc.; 2014. <https://doi.org/10.1016/B978-0-12-396983-5.00022-3>.
23. Chen ZG, Wang PW, Wei B, Mo XM, Cui FZ. Electrospun collagen-chitosan nanofiber: a biomimetic extracellular matrix for endothelial cell and smooth muscle cell. *Acta Biomater* **2010**;6:372–82. <https://doi.org/10.1016/j.actbio.2009.07.024> .
24. Brenner EK, Schiffman JD, Thompson EA, Toth LJ, Schauer CL. Electrospinning of hyaluronic acid nanofibers from aqueous ammonium solutions. *Carbohydr Polym* **2012**;87:926–9. <https://doi.org/10.1016/j.carbpol.2011.07.033> .
25. Jin D, Hu J, Xia D, Liu A, Kuang H, Du J, Mo X, Yin M. Evaluation of a simple off-the-shelf bi-layered vascular scaffold based on poly(L-lactide-co-ε-caprolactone)/silk fibroin in vitro and in vivo. *Int J Nanomed* **2019**;14:4261–76. <https://doi.org/10.2147/IJN.S205569> .
26. Wu T, Zheng H, Chen J, Wang Y, Sun B, Morsi Y, El-Hamshary H, Al-Deyab SS, Chen C, Mo X. Application of a bilayer tubular scaffold based on electrospun poly(l-lactide-co-caprolactone)/collagen fibers and yarns for tracheal tissue engineering. *J Mater Chem B* **2017**;5:139–50. <https://doi.org/10.1039/c6tb02484j> .
27. Panzavolta S, Giofrè M, Focarete ML, Gualandi C, Foroni L, Bigi A. Electrospun gelatin nanofibers: optimization of genipin cross-linking to preserve fiber morphology after exposure to water. *Acta Biomater* **2011**;7:1702–9. <https://doi.org/10.1016/j.actbio.2010.11.021> .
28. Hussey GS, Dziki JL, Badylak SF. Extracellular matrix-based materials for regenerative medicine. *Nat Rev Mater* **2018**;3:159–73. <https://doi.org/10.1038/s41578-018-0023-x> .
29. Huang ZM, Zhang YZ, Kotaki M, Ramakrishna S. A review on polymer nanofibers by electrospinning and their applications in nanocomposites. *Compos Sci Technol* **2003**;63:2223–53. [https://doi.org/10.1016/S0266-3538\(03\)00178-7](https://doi.org/10.1016/S0266-3538(03)00178-7) .
30. Zhou T, Wang N, Xue Y, Ding T, Liu X, Mo X, Sun J. Electrospun tilapia collagen nanofibers accelerating wound healing via inducing keratinocytes proliferation and differentiation. *Colloids Surf B Biointerfaces* **2016**;143:415–22. <https://doi.org/10.1016/j.colsurfb.2016.03.052> .
31. Pang Y, Qin A, Lin X, Yang L, Wang Q, Wang Z, Shan Z, Li S, Wang J, Fan S, Hu Q. Oncotarget 35583 www.impactjournals.com/oncotarget Biodegradable and biocompatible high elastic chitosan scaffold is cell-friendly both in vitro and in vivo. *Oncotarget*. **2017**;8:35583–91.
32. Gurumurthy B, Griggs JA, Janorkar AV. Optimization of collagen-elastin-like polypeptide composite tissue engineering scaffolds using response surface methodology. *J Mech Behav Biomed Mater* **2018**;84:116–25. <https://doi.org/10.1016/j.jmbbm.2018.04.019> .
33. Rad LR, Momeni A, Ghazani BF, Irani M, Mahmoudi M, Noghreh B. Removal of Ni²⁺ and Cd²⁺ ions from aqueous solutions using electrospun PVA/zeolite nanofibrous adsorbent. *Chem Eng J* **2014**;256:119–27. <https://doi.org/10.1016/j.cej.2014.06.066> .
34. Ma J, He Y, Liu X, Chen W, Wang A, Lin CY, Mo X, Ye X. A novel electrospun-aligned nanoyarn/three-dimensional porous nanofibrous hybrid scaffold for annulus fibrosus tissue engineering. *Int J Nanomed* **2018**;13:1553–67. <https://doi.org/10.2147/IJN.S143990> .
35. Zhang K, Fu Q, Yoo J, Chen X, Chandra P, Mo X, Song L, Atala A, Zhao W. 3D bioprinting of urethra with PCL/PLCL blend and dual autologous cells in fibrin hydrogel: an in vitro evaluation of biomimetic mechanical property and cell growth environment. *Acta Biomater* **2017**;50:154–64. <https://doi.org/10.1016/j.actbio.2016.12.008> .
36. Kuang H, Wang Y, Hu J, Wang C, Lu S, Mo X. A method for preparation of an internal layer of artificial vascular graft co-modified with salvianolic acid B and heparin. *ACS Appl Mater Interfaces* **2018**;10:19365–72. <https://doi.org/10.1021/acsami.8b02602> .
37. Rinoldi C, Kijeńska E, Chlanda A, Choinska E, Khenoussi N, Tamayol A, Khademhosseini A, Swieszkowski W. Nanobead-on-string composites for tendon tissue engineering. *J Mater Chem B* **2018**;6:3116–27. <https://doi.org/10.1039/c8tb00246k> .
38. Xue J, Wu T, Dai Y, Xia Y. Electrospinning and electrospun nanofibers: methods, materials, and applications. *Chem Rev* **2019**;119:5298–415. <https://doi.org/10.1021/acs.chemrev.8b00593> .
39. Huang W, Xiao Y, Shi X. Construction of electrospun organic/inorganic hybrid nanofibers for drug delivery and tissue

- engineering applications. *Adv Fiber Mater* **2019**;1:32–45. <https://doi.org/10.1007/s42765-019-00007-w>.
40. Heuer-Jungemann A, Feliu N, Bakaimi I, Hamaly M, Alkilany A, Chakraborty I, Masood A, Casula MF, Kostopoulou A, Oh E, Susumu K, Stewart MH, Medintz IL, Stratakis E, Parak WJ, Kanaras AG. The role of ligands in the chemical synthesis and applications of inorganic nanoparticles. *Chem Rev* **2019**;119:4819–80. <https://doi.org/10.1021/acs.chemrev.8b00733>.
 41. Bose S, Tarafder S. Calcium phosphate ceramic systems in growth factor and drug delivery for bone tissue engineering: a review. *Acta Biomater* **2012**;8:1401–21. <https://doi.org/10.1016/j.actbio.2011.11.017>.
 42. Hossain KMZ, Patel U, Ahmed I. Development of microspheres for biomedical applications: a review. *Prog Biomater* **2015**;4:1–19. <https://doi.org/10.1007/s40204-014-0033-8>.
 43. Denry I, Kuhn LT. Design and characterization of calcium phosphate ceramic scaffolds for bone tissue engineering. *Dent Mater* **2016**;32:43–53. <https://doi.org/10.1016/j.dental.2015.09.008>.
 44. Poologasundarampillai G, Wang D, Li S, Nakamura J, Bradley R, Lee PD, Stevens MM, McPhail DS, Kasuga T, Jones JR. Cotton-wool-like bioactive glasses for bone regeneration. *Acta Biomater* **2014**;10:3733–46. <https://doi.org/10.1016/j.actbio.2014.05.020>.
 45. Liang R, Zhao J, Li B, Cai P, Loh XJ, Xu C, Chen P, Kai D, Zheng L. Implantable and degradable antioxidant poly(ϵ -caprolactone)-lignin nanofiber membrane for effective osteoarthritis treatment. *Biomaterials* **2020**;230:119601. <https://doi.org/10.1016/j.biomaterials.2019.119601>.
 46. Ponnusamy VK, Nguyen DD, Dharmaraja J, Shobana S, Banu JR, Saratale RG, Chang SW, Kumar G. A review on lignin structure, pretreatments, fermentation reactions and biorefinery potential. *Bioresour Technol* **2019**;271:462–72. <https://doi.org/10.1016/j.biortech.2018.09.070>.
 47. Wang C, Kelley SS, Venditti RA. Lignin-based thermoplastic materials. *Chemsuschem* **2016**;9:770–83. <https://doi.org/10.1002/cssc.201501531>.
 48. Wang Z, Lin M, Xie Q, Sun H, Huang Y, Zhang DD, Yu Z, Bi X, Chen J, Wang J, Shi W, Gu P, Fan X. Electrospun silk fibroin/poly(lactide-co- ϵ -caprolactone) nanofibrous scaffolds for bone regeneration. *Int J Nanomed* **2016**;11:1483–500. <https://doi.org/10.2147/IJN.S97445>.
 49. Jin HJ, Chen J, Karageorgiou V, Altman GH, Kaplan DL. Human bone marrow stromal cell responses on electrospun silk fibroin mats. *Biomaterials* **2004**;25:1039–47. [https://doi.org/10.1016/S0142-9612\(03\)00609-4](https://doi.org/10.1016/S0142-9612(03)00609-4).
 50. Cai K, Yao K, Lin S, Yang Z, Li X. Poly(D,L-lactic acid) surfaces modified by silk fibroin: effects on the culture of osteoblast in vitro. *Biomaterials* **2002**;23:1153–60.
 51. Sun B, Zhou Z, Li D, Wu T, Zheng H, Liu J, Wang G, Yu Y, Mo X. Polypyrrole-coated poly(l-lactic acid-co- ϵ -caprolactone)/silk fibroin nanofibrous nerve guidance conduit induced nerve regeneration in rat. *Mater Sci Eng C* **2019**;94:190–9. <https://doi.org/10.1016/j.msec.2018.09.021>.
 52. Fomby P, Cherlin AJ, Hadjizadeh A, Doillon CJ, Sueblinvong V, Weiss DJ, Bates JHT, Gilbert T, Liles WC, Lutzko C, Rajagopal J, Prockop DJ, Chambers D, Giangreco A, Keating A, Kotton D, Lelkes PI, Wagner DE, Prockop DJ. Stem cells and cell therapies in lung biology and diseases: Conference report. *Ann Am Thorac Soc* **2010**;12:181–204. <https://doi.org/10.1002/term>.
 53. Huang ZB, Yin GF, Liao XM, Gu JW. Conducting polypyrrole in tissue engineering applications. *Front Mater Sci* **2014**;8:39–45. <https://doi.org/10.1007/s11706-014-0238-8>.
 54. Sun B, Long YZ, Zhang HD, Li MM, Duvail JL, Jiang XY, Yin HL. Advances in three-dimensional nanofibrous macrostructures via electrospinning. *Prog Polym Sci* **2014**;39:862–90. <https://doi.org/10.1016/j.progpolymsci.2013.06.002>.
 55. Blakeney BA, Tambralli A, Anderson JM, Andukuri A, Lim DJ, Dean DR, Jun HW. Cell infiltration and growth in a low density, uncompressed three-dimensional electrospun nanofibrous scaffold. *Biomaterials* **2011**;32:1583–90. <https://doi.org/10.1016/j.biomaterials.2010.10.056>.
 56. Wu T, Huang C, Li D, Yin A, Liu W, Wang J, Chen J, Ei-Hamshary H, Al-Deyab SS, Mo X. A multi-layered vascular scaffold with symmetrical structure by bi-directional gradient electrospinning. *Colloids Surf B Biointerfaces* **2015**;133:179–88. <https://doi.org/10.1016/j.colsurfb.2015.05.048>.
 57. Hu Q, Su C, Zeng Z, Zhang H, Feng R, Feng J, Li S. Fabrication of multilayer tubular scaffolds with aligned nanofibers to guide the growth of endothelial cells. *J Biomater Appl* **2020**;35:553–66. <https://doi.org/10.1177/0885328220935090>.
 58. Wu T, Zhang J, Wang Y, Li D, Sun B, El-Hamshary H, Yin M, Mo X. Fabrication and preliminary study of a biomimetic tri-layer tubular graft based on fibers and fiber yarns for vascular tissue engineering. *Mater Sci Eng C* **2018**;82:121–9. <https://doi.org/10.1016/j.msec.2017.08.072>.
 59. Dias JR, Baptista-Silva S, Sousa A, Oliveira AL, Bártolo PJ, Granja PL. Biomechanical performance of hybrid electrospun structures for skin regeneration. *Mater Sci Eng C* **2018**;93:816–27. <https://doi.org/10.1016/j.msec.2018.08.050>.
 60. Shokrollahi M, Bahrami SH, Nazarpak MH, Solouk A. Multi-layer nanofibrous patch comprising chamomile loaded carboxy-ethyl chitosan/poly(vinyl alcohol) and polycaprolactone as a potential wound dressing. *Int J Biol Macromol* **2020**;147:547–59. <https://doi.org/10.1016/j.ijbiomac.2020.01.067>.
 61. Birhanu G, Tanha S, Akbari Javar H, Seyedjafari E, Zandi-Karimi A, Kiani B, Dehkordi. Dexamethasone loaded multi-layer poly-l-lactic acid/pluronic P123 composite electrospun nanofiber scaffolds for bone tissue engineering and drug delivery. *Pharm Dev Technol* **2019**;24:338–47. <https://doi.org/10.1080/10837450.2018.1481429>.
 62. Aghajanianpoor M, Hashemi-Najafabadi S, Baghaban-Eslaminejad M, Bagheri F, Mohammad Mousavi S, Azam F, Sayyahpour. The effect of increasing the pore size of nanofibrous scaffolds on the osteogenic cell culture using a combination of sacrificial agent electrospinning and ultrasonication. *J Biomed Mater Res Part A* **2017**;105:1887–99. <https://doi.org/10.1002/jbm.a.36052>.
 63. Türker E, Yildiz ÜH, Arslan A, Yildiz. Biomimetic hybrid scaffold consisting of co-electrospun collagen and PLLCL for 3D cell culture. *Int J Biol Macromol* **2019**;139:1054–62. <https://doi.org/10.1016/j.ijbiomac.2019.08.082>.
 64. Hodge J, Quint C. The improvement of cell infiltration in an electrospun scaffold with multiple synthetic biodegradable polymers using sacrificial PEO microparticles. *J Biomed Mater Res Part A* **2019**;107:1954–64. <https://doi.org/10.1002/jbm.a.36706>.
 65. Kishan AP, Cosgriff-Hernandez EM. Recent advancements in electrospinning design for tissue engineering applications: a review. *J Biomed Mater Res Part A* **2017**;105:2892–905. <https://doi.org/10.1002/jbm.a.36124>.
 66. Chen Z, Ma S, Hu Y, Lv F, Zhang Y. Preparation of Bi-based porous and magnetic electrospun fibers and their photocatalytic properties in weak polar medium. *Colloids Surf A Physicochem Eng Asp* **2021**;610:125718. <https://doi.org/10.1016/j.colsurfa.2020.125718>.
 67. Zhou M, Zhou J, Li R, Xie E. Preparation of aligned ultra-long and diameter-controlled silicon oxide nanotubes by plasma enhanced chemical vapor deposition using electrospun pvp nanofiber template. *Nanoscale Res Lett* **2010**;5:279–85. <https://doi.org/10.1007/s11671-009-9476-6>.
 68. Sajedeh K, Atefeh S, Hamid M, Saeedeh M, Jose L, Shahriar MS, Seeram R. A review of key challenges of electrospun scaffolds for tissue-engineering applications. *J Tissue Eng Regen Med* **2016**;10:715–38. <https://doi.org/10.1002/term>.

69. Nosar MN, Salehi M, Ghorbani S, Beiranvand SP, Goodarzi A, Azami M. Characterization of wet-electrospun cellulose acetate based 3-dimensional scaffolds for skin tissue engineering applications: influence of cellulose acetate concentration. *Cellulose* **2016**;23:3239–48. <https://doi.org/10.1007/s10570-016-1026-7>.
70. Kishimoto Y, Kobashi T, Morikawa H, Tamada Y. Production of three-dimensional silk fibroin nanofiber non-woven fabric by wet electrospinning. *J Silk Sci Technol Japan*. **2017**;25:49–57. <https://doi.org/10.11417/silk.25.49>.
71. Wu T, Zhang J, Wang Y, Sun B, Guo X, Morsi Y, El-Hamshary H, El-Newehy M, Mo X. Development of dynamic liquid and conjugated electrospun poly(L-lactide-co-caprolactone)/collagen nanoyarns for regulating vascular smooth muscle cells growth. *J Biomed Nanotechnol* **2017**;13:303–12. <https://doi.org/10.1166/jbn.2017.2352>.
72. Sun B, Li J, Liu W, Aqeel BM, El-Hamshary H, Al-Deyab SS, Mo X. Fabrication and characterization of mineralized P(LLA-CL)/SF three-dimensional nanoyarn scaffolds. *Iran Polym J (English Ed)*. **2015**;24:29–40. <https://doi.org/10.1007/s13726-014-0297-9>.
73. Farzambar S, Naseri-Nosar M, Vaez A, Esmailpour F, Ehterami A, Sahrapeyma H, Samadian H, Hamidieh AA, Ghorbani S, Goodarzi A, Azami A, Salehi M. Neural tissue regeneration by a gabapentin-loaded cellulose acetate/gelatin wet-electrospun scaffold. *Cellulose* **2018**;25:1229–38. <https://doi.org/10.1007/s10570-017-1632-z>.
74. Wu J, Hong Y. Enhancing cell infiltration of electrospun fibrous scaffolds in tissue regeneration. *Bioact Mater* **2016**;1:56–64. <https://doi.org/10.1016/j.bioactmat.2016.07.001>.
75. Wu J, Huang C, Liu W, Yin A, Chen W, He C, Wang H, Liu S, Fan C, Bowlin GL, Mo X. Cell infiltration and vascularization in porous nanoyarn scaffolds prepared by dynamic liquid electrospinning. *J Biomed Nanotechnol* **2014**;10:603–14. <https://doi.org/10.1166/jbn.2014.1733>.
76. Nieminen HJ, Laidmäe I, Salmi A, Rauhala T, Paulin T, Heinämäki J, Hæggröm E. Ultrasound-enhanced electrospinning. *Sci Rep* **2018**;8:1–6. <https://doi.org/10.1038/s41598-018-22124-z>.
77. Partheniadis I, Nikolakakis I, Laidmäe I, Heinämäki J. A mini-review: needleless electrospinning of nanofibers for pharmaceutical and biomedical applications. *Processes* **2020**;8:673. <https://doi.org/10.3390/PR8060673>.
78. Hakkarainen E, Kõrkjas A, Laidmäe I, Lust A, Semjonov K, Kogermann K, Nieminen HJ, Salmi A, Korhonen O, Haeggström E, Heinämäki J. Comparison of traditional and ultrasound-enhanced electrospinning in fabricating nanofibrous drug delivery systems. *Pharmaceutics* **2019**;11:1–10. <https://doi.org/10.3390/pharmaceutics11100495>.
79. Badami AS, Kreke MR, Thompson MS, Riffle JS, Goldstein AS. Effect of fiber diameter on spreading, proliferation, and differentiation of osteoblastic cells on electrospun poly(lactic acid) substrates. *Biomaterials* **2006**;27:596–606. <https://doi.org/10.1016/j.biomaterials.2005.05.084>.
80. Partheniadis I, Athanasiou K, Laidmäe I, Heinämäki J, Nikolakakis I. Physicomechanical characterization and tablet compression of theophylline nanofibrous mats prepared by conventional and ultrasound enhanced electrospinning. *Int J Pharm* **2022**;616:121558. <https://doi.org/10.1016/j.ijpharm.2022.121558>.
81. Chen Y, Xu W, Shafiq M, Tang J, Hao J, Xie X, Yuan Z, Xiao X, Liu Y, Mo X. Three-dimensional porous gas-foamed electrospun nanofiber scaffold for cartilage regeneration. *J Colloid Interface Sci* **2021**;603:94–109. <https://doi.org/10.1016/j.jcis.2021.06.067>.
82. Chen Y, Jia Z, Shafiq M, Xie X, Xiao X, Castro R, Rodrigues J, Wu J, Zhou G, Mo X. Gas foaming of electrospun poly(L-lactide-co-caprolactone)/silk fibroin nanofiber scaffolds to promote cellular infiltration and tissue regeneration. *Colloids Surf B Biointerfaces*. **2021**;201:111637. <https://doi.org/10.1016/j.colsurfb.2021.111637>.
83. Pina S, Oliveira JM, Reis RL. Natural-based nanocomposites for bone tissue engineering and regenerative medicine: A review. *Adv Mater* **2015**;27:1143–69. <https://doi.org/10.1002/adma.201403354>.
84. Lin W, Chen M, Qu T, Li J, Man Y. Three-dimensional electrospun nanofibrous scaffolds for bone tissue engineering. *J Biomed Mater Res Part B Appl Biomater*. **2020**;108:1311–21. <https://doi.org/10.1002/jbm.b.34479>.
85. Joshi MK, Pant HR, Tiwari AP, Kim HJ, Park CH, Kim CS. Multi-layered macroporous three-dimensional nanofibrous scaffold via a novel gas foaming technique. *Chem Eng J*. **2015**;275:79–88. <https://doi.org/10.1016/j.cej.2015.03.121>.
86. Jiang J, Carlson MA, Teusink MJ, Wang H, MacEwan MR, Xie J. Expanding two-dimensional electrospun nanofiber membranes in the third dimension by a modified gas-foaming technique. *ACS Biomater Sci Eng* **2015**;1:991–1001. <https://doi.org/10.1021/acsbomaterials.5b00238>.
87. Jiang J, Li Z, Wang H, Wang Y, Carlson MA, Teusink MJ, MacEwan MR, Gu L, Xie J. Expanded 3D nanofiber scaffolds: cell penetration, neovascularization, and host response. *Adv Healthc Mater* **2016**;5:2993–3003. <https://doi.org/10.1002/adhm.201608080>.
88. Gao Q, Gu H, Zhao P, Zhang C, Cao M, Fu J, He Y. Fabrication of electrospun nanofibrous scaffolds with 3D controllable geometric shapes. *Mater Des* **2018**;157:159–69. <https://doi.org/10.1016/j.matdes.2018.07.042>.
89. Jing X, Li H, Mi HY, Liu YJ, Tan YM. Fabrication of fluffy shish-kebab structured nanofibers by electrospinning. CO₂ escaping foaming and controlled crystallization for biomimetic tissue engineering scaffolds. *Chem Eng J* **2019**;372:785–95. <https://doi.org/10.1016/j.cej.2019.04.194>.
90. Jiang J, Chen S, Wang H, Carlson MA, Gombart AF, Xie J. CO₂-expanded nanofiber scaffolds maintain activity of encapsulated bioactive materials and promote cellular infiltration and positive host response. *Acta Biomater* **2018**;68:237–48. <https://doi.org/10.1016/j.actbio.2017.12.018>.
91. Zhang K, Bai X, Yuan Z, Cao X, Jiao X, Li Y, Qin Y, Wen Y, Zhang X. Layered nanofiber sponge with an improved capacity for promoting blood coagulation and wound healing. *Biomaterials* **2019**;204:70–9. <https://doi.org/10.1016/j.biomaterials.2019.03.008>.
92. Rao F, Yuan Z, Li M, Yu F, Fang X, Jiang B, Wen Y, Zhang P. Expanded 3D nanofiber sponge scaffolds by gas-foaming technique enhance peripheral nerve regeneration. *Artif Cells, Nanomedicine, Biotechnol* **2019**;47:491–500. <https://doi.org/10.1080/21691401.2018.1557669>.
93. Chen Y, Xu W, Shafiq M, Song D, Xie X, Yuan Z, El-Newehy M, El-Hamshary H, Morsi Y, Liu Y, Mo X. Chondroitin sulfate cross-linked three-dimensional tailored electrospun scaffolds for cartilage regeneration. *Mater Sci Eng C*. **2022**. <https://doi.org/10.1016/j.msec.2022.112643>.
94. Kim SE, Tiwari AP. Three dimensional polycaprolactone/cellulose scaffold containing calcium-based particles: a new platform for bone regeneration. *Carbohydr Polym* **2020**;250:116880. <https://doi.org/10.1016/j.carbpol.2020.116880>.
95. Lee JB, Jeong SI, Bae MS, Yang DH, Heo DN, Kim CH, Alsberg E, Kwon IK. Highly porous electrospun nanofibers enhanced by ultrasonication for improved cellular infiltration. *Tissue Eng Part A* **2011**;17:2695–702. <https://doi.org/10.1089/ten.tea.2010.0709>.
96. Jeong SI, Burns NA, Bonino CA, Kwon IK, Khan SA, Alsberg E. Improved cell infiltration of highly porous 3D nanofibrous

- scaffolds formed by combined fiber-fiber charge repulsions and ultra-sonication. *J Mater Chem B* **2014**;2:8116–22. <https://doi.org/10.1039/c4tb01487a> .
97. Rahmani A, Hashemi-Najafabadi S, Eslaminejad MB, Bagheri F, Sayahpour FA. The effect of modified electrospun PCL-nHA-nZnO scaffolds on osteogenesis and angiogenesis. *J Biomed Mater Res Part A* **2019**;107:2040–52. <https://doi.org/10.1002/jbm.a.36717> .
 98. Ahtzaz S, Nasir M, Shahzadi L, Iqbal F, Chaudhry AA, Yar M, Ur Rehman I, Amir W, Anjum A, Arshad R. A study on the effect of zinc oxide and zinc peroxide nanoparticles to enhance angiogenesis-pro-angiogenic grafts for tissue regeneration applications. *Mater Des*. **2017**;132:409–18. <https://doi.org/10.1016/j.matdes.2017.07.023> .
 99. Laurenti M, Cauda V. ZnO nanostructures for tissue engineering applications. *Nanomaterials* **2017**;7:374. <https://doi.org/10.3390/nano7110374> .
 100. Chen W, Ma J, Zhu L, Morsi Y, El-hamshary H, Al-deyab SS, Mo X. Superelastic, superabsorbent and 3D nanofiber-assembled scaffold for tissue engineering. *Colloids Surf B Biointerfaces* **2016**;142:165–72. <https://doi.org/10.1016/j.colsurfb.2016.02.050> .
 101. Chen W, Chen S, Morsi Y, El-Hamshary H, El-Newhy M, Fan C, Mo X. Superabsorbent 3D scaffold based on electrospun nanofibers for cartilage tissue engineering. *ACS Appl Mater Interfaces* **2016**;8:24415–25. <https://doi.org/10.1021/acsami.6b06825> .
 102. Ye K, Liu D, Kuang H, Cai J, Chen W, Sun B, Xia L, Fang B, Morsi Y, Mo X. Three-dimensional electrospun nanofibrous scaffolds displaying bone morphogenetic protein-2-derived peptides for the promotion of osteogenic differentiation of stem cells and bone regeneration. *J Colloid Interface Sci* **2019**;534:625–36. <https://doi.org/10.1016/j.jcis.2018.09.071> .
 103. Mader M, Jérôme V, Freitag R, Agarwal S, Greiner A. Ultraporous, compressible, wettable polylactide/polycaprolactone sponges for tissue engineering. *Biomacromol* **2018**;19:1663–73. <https://doi.org/10.1021/acs.biomac.8b00434> .
 104. Chen S, Chen W, Chen Y, Mo X, Fan C. Chondroitin sulfate modified 3D porous electrospun nanofiber scaffolds promote cartilage regeneration. *Mater Sci Eng C* **2021**;118:1–12. <https://doi.org/10.1016/j.msec.2020.111312> .
 105. Sutherland AJ, Converse GL, Hopkins RA, Detamore MS. The bioactivity of cartilage extracellular matrix in articular cartilage regeneration. *Adv Healthc Mater* **2015**;4:29–39. <https://doi.org/10.1002/adhm.201400165> .
 106. Almeida HV, Liu Y, Cuniffe GM, Mulhall KJ, Matsiko A, Buckley CT, O'Brien FJ, Kelly DJ. Controlled release of transforming growth factor- β 3 from cartilage-extra-cellular-matrix-derived scaffolds to promote chondrogenesis of human-joint-tissue-derived stem cells. *Acta Biomater* **2014**;10:4400–9. <https://doi.org/10.1016/j.actbio.2014.05.030> .
 107. Li Y, Liu Y, Xun X, Zhang W, Xu Y, Gu D. Three-dimensional porous scaffolds with biomimetic microarchitecture and bioactivity for cartilage tissue engineering. *ACS Appl Mater Interfaces* **2019**;11:36359–70. <https://doi.org/10.1021/acsami.9b12206> .
 108. Shen Y, Xu Y, Yi B, Wang X, Tang H, Chen C, Zhang Y. Engineering a highly biomimetic chitosan-based cartilage scaffold by using short fibers and a cartilage-decellularized matrix. *Biomacromol* **2021**;22:2284–97. <https://doi.org/10.1021/acs.biomac.1c00366> .
 109. Wang L, Qiu Y, Guo Y, Si Y, Liu L, Cao J, Yu J, Li X, Zhang Q, Ding B. Smart, elastic, and nanofiber-based 3D scaffolds with self-deploying capability for osteoporotic bone regeneration. *Nano Lett* **2019**;19:9112–20. <https://doi.org/10.1021/acs.nanolett.9b04313> .
 110. Liu X, Chen M, Luo J, Zhao H, Zhou X, Gu Q, Yang H, Zhu X, Cui W, Shi Q. Immunopolarization-regulated 3D printed-electrospun fibrous scaffolds for bone regeneration. *Biomaterials* **2021**;276:121037. <https://doi.org/10.1016/j.biomaterials.2021.121037> .
 111. Chen W, Xu Y, Liu Y, Wang Z, Li Y, Jiang G, Mo X, Zhou G. Three-dimensional printed electrospun fiber-based scaffold for cartilage regeneration. *Mater Des* **2019**;179:107886. <https://doi.org/10.1016/j.matdes.2019.107886> .
 112. Chen W, Xu Y, Li Y, Jia L, Mo X, Jiang G, Zhou G. 3D printing electrospinning fiber-reinforced decellularized extracellular matrix for cartilage regeneration. *Chem Eng J* **2020**;382:122986. <https://doi.org/10.1016/j.cej.2019.122986> .
 113. Yuan Z, Ren Y, Shafiq M, Chen Y, Tang H, Li B, El-Newehy M, El-hamshary H, Morsi Y, Zheng H, Mo X. Converging 3D printing and electrospinning: effect of poly(L-lactide)/gelatin based short nanofibers aerogels on tracheal regeneration. *Macromol Biosci*. **2021**;2100342:2100342. <https://doi.org/10.1002/mabi.202100342> .
 114. Huttmacher DW, Schantz T, Zein I, Ng KW, Teoh SH, Tan KC. Mechanical properties and cell cultural response of polycaprolactone scaffolds designed and fabricated via fused deposition modeling. *J Biomed Mater Res* **2001**;55:203–16. [https://doi.org/10.1002/1097-4636\(200105\)55:2%3c203::AID-JBM1007%3e3.0.CO;2-7](https://doi.org/10.1002/1097-4636(200105)55:2%3c203::AID-JBM1007%3e3.0.CO;2-7) .
 115. Naghieh S, Foroozmehr E, Badrossamay M, Kharaziha M. Combinational processing of 3D printing and electrospinning of hierarchical poly(lactic acid)/gelatin-forsterite scaffolds as a biocomposite: mechanical and biological assessment. *Mater Des* **2017**;133:128–35. <https://doi.org/10.1016/j.matdes.2017.07.051> .
 116. Chen W, Xu Y, Liu Y, Wang Z, Li Y, Jiang G, Mo X, Zhou G. Three-dimensional printed electrospun fiber-based scaffold for cartilage regeneration. *Mater Des*. **2019**. <https://doi.org/10.1016/j.matdes.2019.107886> .
 117. Boda SK, Chen S, Chu K, Kim HJ, Xie J. Electrospinning electrospun nanofiber segments into injectable microspheres for potential cell delivery. *ACS Appl Mater Interfaces* **2018**;10:25069–79. <https://doi.org/10.1021/acsami.8b06386> .
 118. Yi B, Zhang H, Yu Z, Yuan H, Wang X, Zhang Y. Fabrication of high performance silk fibroin fibers: via stable jet electrospinning for potential use in anisotropic tissue regeneration. *J Mater Chem B* **2018**;6:3934–45. <https://doi.org/10.1039/c8tb00535d> .
 119. Shen Y, Tu T, Yi B, Wang X, Tang H, Liu W, Zhang Y. Electrospun acid-neutralizing fibers for the amelioration of inflammatory response. *Acta Biomater* **2019**;97:200–15. <https://doi.org/10.1016/j.actbio.2019.08.014> .
 120. Zhang Z, Eyster TW, Ma PX. Nanostructured injectable cell microcarriers for tissue regeneration. *Nanomedicine* **2016**;11:1611–28. <https://doi.org/10.2217/nmm-2016-0083> .
 121. Liu X, Jin X, Ma PX. Nanofibrous hollow microspheres self-assembled from star-shaped polymers as injectable cell carriers for knee repair. *Nat Mater* **2011**;10:398–406. <https://doi.org/10.1038/nmat2999> .
 122. John JV, Choksi M, Chen S, Boda SK, Su Y, McCarthy A, Teusink MJ, Reinhardt RA, Xie J. Tethering peptides onto biomimetic and injectable nanofiber microspheres to direct cellular response. *Nanomed Nanotechnol Biol Med* **2019**;22:102081. <https://doi.org/10.1016/j.nano.2019.102081> .
 123. Zhang B, Gao Y, Yang R, Ouyang Z, Yu H, Wang H, Shi X, Shen M. Tumor-anchoring drug-loaded fibrous microspheres for mr imaging-guided local chemotherapy and metastasis inhibition. *Adv Fiber Mater* **2022**. <https://doi.org/10.1007/s42765-022-00137-8> .
 124. John JV, McCarthy A, Wang H, Chen S, Su Y, Davis E, Li X, Park JS, Reinhardt RA, Xie J. Engineering biomimetic nanofiber microspheres with tailored size, predesigned structure, and desired composition via gas bubble-mediated coaxial

- electrospray. *Small*. **2020**. <https://doi.org/10.1002/sml.201907393>.
125. Yuan H, Zhao S, Tu H, Li B, Li Q, Feng B, Peng H, Zhang Y. Stable jet electrospinning for easy fabrication of aligned ultrafine fibers. *J Mater Chem* **2012**;22:19634–8. <https://doi.org/10.1039/c2jm33728b>.
 126. Lian M, Han Y, Sun B, Xu L, Wang X, Ni B, Jiang W, Qiao Z, Dai K, Zhang X. A multifunctional electrowritten bi-layered scaffold for guided bone regeneration. *Acta Biomater* **2020**;118:83–99. <https://doi.org/10.1016/j.actbio.2020.08.017>.
 127. Qiao Z, Lian M, Han Y, Sun B, Zhang X, Jiang W, Li H, Hao Y, Dai K. Bioinspired stratified electrowritten fiber-reinforced hydrogel constructs with layer-specific induction capacity for functional osteochondral regeneration. *Biomaterials* **2021**;266:120385. <https://doi.org/10.1016/j.biomaterials.2020.120385>.
 128. Han Y, Jia B, Lian M, Sun B, Wu Q, Sun B, Qiao Z, Dai K. High-precision, gelatin-based, hybrid, bilayer scaffolds using melt electro-writing to repair cartilage injury. *Bioact Mater* **2021**;6:2173–86. <https://doi.org/10.1016/j.bioactmat.2020.12.018>.
 129. Han Y, Lian M, Sun B, Jia B, Wu Q, Qiao Z, Dai K. Preparation of high precision multilayer scaffolds based on Melt Electro-Writing to repair cartilage injury. *Theranostics* **2020**;10:10214–30. <https://doi.org/10.7150/thno.47909>.
 130. Xu Y, Duan L, Li Y, She Y, Zhu J, Zhou G, Jiang G, Yang Y. Nanofibrillar decellularized Wharton's jelly matrix for segmental tracheal repair. *Adv Funct Mater* **2020**;30:1910067. <https://doi.org/10.1002/adfm.201910067>.
 131. John JV, McCarthy A, Wang H, Luo Z, Li H, Wang Z, Cheng F, Zhang YS, Xie J. Freeze-casting with 3D-printed templates creates anisotropic microchannels and patterned macrochannels within biomimetic nanofiber aerogels for rapid cellular infiltration. *Adv Healthc Mater* **2021**;2100238:2100238. <https://doi.org/10.1002/adhm.202100238>.
 132. Zhang K, Jiao X, Zhou L, Wang J, Wang C, Qin Y, Wen Y. Biomaterials nanofibrous composite aerogel with multi-bioactive and fluid gating characteristics for promoting diabetic wound healing. *Biomaterials* **2021**;276:121040. <https://doi.org/10.1016/j.biomaterials.2021.121040>.
 133. Orr SB, Chainani A, Hippensteel KJ, Kishan A, Gilchrist C, Garrigues NW, Ruch DS, Guilak F, Little D. Aligned multilayered electrospun scaffolds for rotator cuff tendon tissue engineering. *Acta Biomater* **2015**;24:117–26. <https://doi.org/10.1016/j.actbio.2015.06.010>.
 134. Zhang K, Cao N, Guo X, Zou Q, Zhou S, Yang R, Zhao W, Mo X, Liu W, Fu Q. The fabrication of 3D surface scaffold of collagen/poly (L-lactide-co-caprolactone) with dynamic liquid system and its application in urinary incontinence treatment as a tissue engineered sub-urethral sling: in vitro and in vivo study. *Neurourol Urodyn* **2018**;37:978–85. <https://doi.org/10.1002/nau.23438>.
 135. Salehi M, Naseri-Nosar M, Azami M, Nodooshan SJ, Arish J. Comparative study of poly(L-lactic acid) scaffolds coated with chitosan nanoparticles prepared via ultrasonication and ionic gelation techniques. *Tissue Eng Regen Med* **2016**;13:498–506. <https://doi.org/10.1007/s13770-016-9083-4>.
 136. Kurpinski KT, Stephenson JT, Janairo RRR, Lee H, Li S. The effect of fiber alignment and heparin coating on cell infiltration into nanofibrous PLLA scaffolds. *Biomaterials* **2010**;31:3536–42. <https://doi.org/10.1016/j.biomaterials.2010.01.062>.
 137. Sell SA, Wolfe PS, Ericksen JJ, Simpson DG, Bowlin GL. Incorporating platelet-rich plasma into electrospun scaffolds for tissue engineering applications. *Tissue Eng Part A* **2011**;17:2723–37. <https://doi.org/10.1089/ten.tea.2010.0663>.
 138. Yuan Z, Sheng D, Jiang L, Shafiq M, A ur R Khan, Hashim R, Chen Y, Li B, Xie X, Chen J, Morsi Y, Mo X, Chen S. Vascular endothelial growth factor-capturing aligned electrospun polycaprolactone/gelatin nanofibers promote patellar ligament regeneration. *Acta Biomater*. **2022**;140:233–246. <https://doi.org/10.1016/j.actbio.2021.11.040>.
 139. Stylianopoulos T, Bashur CA, Goldstein AS, Guelcher SA, Barocas VH. Computational predictions of the tensile properties of electrospun fibre meshes: effect of fibre diameter and fibre orientation. *J Mech Behav Biomed Mater* **2008**;1:326–35. <https://doi.org/10.1016/j.jmbbm.2008.01.003>.
 140. Lannutti J, Reneker D, Ma T, Tomasko D, Farson D. Electrospinning for tissue engineering scaffolds. *Mater Sci Eng C* **2007**;27:504–9. <https://doi.org/10.1016/j.msec.2006.05.019>.
 141. Yang Z, Peng H, Wang W, Liu T. Crystallization behavior of poly(ϵ -caprolactone)/layered double hydroxide nanocomposites. *J Appl Polym Sci* **2010**;116:2658–67. <https://doi.org/10.1002/app>.

Publisher's note Springer Nature remains neutral with regard to jurisdictional claims in published maps and institutional affiliations.



Yujie Chen obtained his B.S. degree in Polymer Materials and Engineering from Jiaying University in 2018. Currently, he is a Ph.D. candidate in the College of Chemistry, Chemical Engineering and Biotechnology, Donghua University, supervised by Prof. Xiumei Mo. His research interests are focused on 3D electrospun nanofiber scaffolds and their applications for cartilage regeneration.



Xutao Dong graduated from The University of Edinburgh with BEng (Hons) in Chemical Engineering and graduated from University College London with MSc in Advanced Materials Science (Energy Storage). Currently, she is waiting to start as a graduate in institutional banking.



Dr. Muhammad Shafiq has received his BS and MS degrees both from Pakistan. In 2018, Dr. Shafiq received his Ph.D. degree (summa cum laude) in Biomedical Engineering from University of Science & Technology (UST), South Korea while working under the mentorship of Dr. Soo Hyun Kim. He is now an Assistant Professor at the Department of Chemistry, PIEAS, Islamabad, Pakistan working in the field of polymeric biomaterials, self-assembled materials, and nanostructured materials for

stem cell bioengineering, regenerative medicine, and tissue engineering as well as environmental remediation. Dr. Shafiq has authored over 30 peer-reviewed papers and 2 book chapters. He has been conferred with several prizes, awards, and honors including TERMIS-AP student travel award and Grand Prize from UST, academic excellence award from KIST, South Korea, and Research Productivity Award from Pakistan Council for Science & Technology.



Gregory Myles is a PhD candidate in the Centre for Doctoral Training in Intelligent Sensing and Measurement (CDT-ISM) at the University of Edinburgh. Building upon a foundation in clinical medicine, his current research interests lie in the development of optical nanosensors for the continuous monitoring of cancerous tumors.



Dr. Norbert Radacsi is a Senior Lecturer in Chemical Engineering and director of the NanoMaterials Laboratory at The University of Edinburgh. He obtained his Ph.D. at the Delft University

of Technology in chemical engineering. Then he was postdoctoral researcher at Purdue University and California Institute of Technology. He has published over 50 articles in international journals and pioneered a new type of 3D electrospinning technology. His research focuses on advancing electrospinning technology and bioprinting.



Dr. Xiumei Mo is a professor at Donghua University. She once had two years of Postdoc experience at Kyoto University, three years of research fellow experience at the National University of Singapore, a one-year visiting professor experience at Aachen University of Applied Science and Technology. In Donghua University, she was granted 30 more projects related to nanofiber fabrication for different tissue regeneration. She has published more than 400 papers.

ISI Web of Science shows that her publication related to electrospinning is ranked No.7 in the world. She got the Science Technical Invention Awards from Shanghai Municipality in 2008, Science and Technology Progress Awards from the State Department of People's Republic of China in 2009, Nature Science Awards from Shanghai Government in 2015. She is the committee member of China Biomaterials Society as well as the Biomedical Engineering Society Biomaterials Branch.